

**Titre:** Uncovering and leveraging the return of voluntary motor programs after paralysis using a bi-cortical neuroprosthesis

**Auteurs:** Maude Duguay, Marco Bonizzato, Hugo Delivet-Mongrain, Nicolas Fortier-Lebel, & Marina Martinez

**Date:** 2023

**Type:** Article de revue / Article

**Référence:** Duguay, M., Bonizzato, M., Delivet-Mongrain, H., Fortier-Lebel, N., & Martinez, M. (2023). Uncovering and leveraging the return of voluntary motor programs after paralysis using a bi-cortical neuroprosthesis. Progress in Neurobiology, 228, 102492 (15 pages). <https://doi.org/10.1016/j.pneurobio.2023.102492>

## Document en libre accès dans PolyPublie

Open Access document in PolyPublie

**URL de PolyPublie:** <https://publications.polymtl.ca/54361/>

PolyPublie URL:

**Version:** Version officielle de l'éditeur / Published version  
Révisé par les pairs / Refereed

**Conditions d'utilisation:** CC BY-NC-ND

Terms of Use:

## Document publié chez l'éditeur officiel

Document issued by the official publisher

**Titre de la revue:** Progress in Neurobiology (vol. 228)

Journal Title:

**Maison d'édition:** Elsevier BV

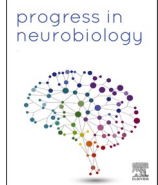
Publisher:

**URL officiel:** <https://doi.org/10.1016/j.pneurobio.2023.102492>

Official URL:

**Mention légale:** © 2023 The Author(s). Published by Elsevier Ltd. This is an open access article under the CC BY-NC-ND license (<http://creativecommons.org/licenses/by-nc-nd/4.0/>).

Legal notice:



# Uncovering and leveraging the return of voluntary motor programs after paralysis using a bi-cortical neuroprosthesis

Maude Duguay<sup>a,b,1</sup>, Marco Bonizzato<sup>a,b,c,1</sup>, Hugo Delivet-Mongrain<sup>a</sup>, Nicolas Fortier-Lebel<sup>a</sup>, Marina Martinez<sup>a,b,\*</sup>

<sup>a</sup> Département de Neurosciences and Centre interdisciplinaire de recherche sur le cerveau et l'apprentissage (CIRCA), Université de Montréal, Québec, Canada

<sup>b</sup> CIUSSS du Nord-de-l'Île-de-Montréal, Québec, Canada

<sup>c</sup> Department of Electrical Engineering, Polytechnique Montréal, Québec, Canada

## ARTICLE INFO

### Keywords:

Neuroprosthetics  
Cortical stimulation  
Locomotion  
Cat  
Spinal cord injury  
Recovery  
Plasticity

## ABSTRACT

Rehabilitative and neuroprosthetic approaches after spinal cord injury (SCI) aim to reestablish voluntary control of movement. Promoting recovery requires a mechanistic understanding of the return of volition over action, but the relationship between re-emerging cortical commands and the return of locomotion is not well established. We introduced a neuroprosthesis delivering targeted bi-cortical stimulation in a clinically relevant contusive SCI model. In healthy and SCI cats, we controlled hindlimb locomotor output by tuning stimulation timing, duration, amplitude, and site. In intact cats, we unveiled a large repertoire of motor programs. After SCI, the evoked hindlimb lifts were highly stereotyped, yet effective in modulating gait and alleviating bilateral foot drag. Results suggest that the neural substrate underpinning motor recovery had traded-off selectivity for efficacy. Longitudinal tests revealed that the return of locomotion after SCI was correlated with recovery of the descending drive, which advocates for rehabilitation interventions directed at the cortical target.

## 1. Introduction

Vertebrate locomotion is controlled by the following mechanisms: (1) integrated spinal central pattern generators (CPGs) that establish motor rhythms (Barbeau and Rossignol, 1987; D'Angelo et al., 2014; Frigon et al., 2017; Frigon et al., 2015; Grillner and Zangger, 1979; Kiehn, 2006); (2) sensory feedback, which is a reaction to environmental perturbations (Prochazka et al., 2002; Rossignol et al., 2006; Zehr and Stein, 1999); and (3) supraspinal commands, which are involved in locomotion initiation and modulation as well as balance and voluntary control of movement (Drew et al., 2002; Fortier-Lebel et al., 2021; Jordan et al., 2008).

Among supraspinal contributors, the motor cortex is a key player in the execution and voluntary control of hindlimb movements, which has been dissected through various lesion (Jiang and Drew, 1996; Metz et al., 1998) and recording studies (DiGiovanna et al., 2016; Sahrmann et al., 1984; Widajewicz et al., 1994). In anesthetized preparations, intracortical microstimulation (ICMS) of the motor cortex evokes simple

hindlimb movements (Brown and Martinez, 2018; Hatanaka et al., 2001; Neafsey et al., 1986; Seong et al., 2014). In healthy conscious rats and cats, the application of ICMS during locomotion produces phase-dependent contralateral movements through direct and indirect projections to the spinal cord (Bonizzato and Martinez, 2021; Bretzner and Drew, 2005b; Fortier-Lebel et al., 2021).

Disruption of descending projections due to spinal cord injury (SCI) induces paralysis and loss of locomotor control, whose recovery is a high priority for individuals with lived experience (Ditunno et al., 2008). SCI in humans primarily results from contusions and induces variable spinal tract damage that impairs residual pathway functionality (Ahuja et al., 2017; RHI, 2018). Since 70 % of contusive SCIs are incomplete (N.S.C.I. S.C., 2019; RHI, 2018), supraspinal centers often retain connections with spinal circuits. Although the neuroplasticity of lumbar spinal networks may support the return of locomotor rhythms (Barbeau and Rossignol, 1987), sufficient sparing of descending tracts is required for functional return of volitional walking (Delivet-Mongrain et al., 2020; Jiang and Drew, 1996). Motor cortex plasticity plays a prominent role in the

\* Corresponding author at: Département de neurosciences, Faculté de médecine, Université de Montréal, C.P. 6128, Succ. Centre-ville, Montréal, Québec H3C 3J7, Canada.

E-mail address: [marina.martinez@umontreal.ca](mailto:marina.martinez@umontreal.ca) (M. Martinez).

<sup>1</sup> These authors equally contributed to this work.

recovery of voluntary leg control (Bonizzato and Martinez, 2021; Brown and Martinez, 2018; Brown and Martinez, 2021; Topka et al., 1991; Urbin et al., 2019), although the cortical contribution to recovery from severe contusion in clinically relevant animal models remains poorly understood. In a rat model of thoracic hemisection with paralysis of one leg, we showed that ICMS delivered in phase coherence with ongoing locomotion immediately restored locomotion (Bonizzato and Martinez, 2021; Martinez, 2022). However, the utility of neuromodulation strategies targeting the motor cortex to immediately restore bilateral control of locomotion after severe contusions is unknown.

To address this knowledge gap, we designed a neuroprosthetic platform whereby ICMS was delivered alternately to the left and right motor cortex during ongoing locomotion. In healthy cats, we extensively characterized the impact of varying stimulation parameters (timing, duration, amplitude, and site of stimulation) on locomotor output. When delivered at the initiation of the leg flexion phase of locomotion (in “phase coherence” with locomotion), ICMS evoked a variety of motor synergies. After contusive SCI that initially paralyzed both legs, bi-cortical stimulation immediately reversed bilateral foot drag and flexion deficits. We also demonstrated that the return of cortically evoked movements simultaneously occurred with the recovery of voluntary motor control. Our data provide a proof-of-concept methodology to independently modulate bilateral limb trajectories, scrutinizing the level, variety, and timeline of cortical control of movement expression. Overall, this study provides the building blocks for stimulation protocols to control and improve gait following severe SCI.

## 2. Materials and methods

### 2.1. Study design

The objective of this research was to determine the immediate effects of ICMS on locomotor output under intact conditions and after a spinal contusion. Three female tabby cats (one-year-old; MBR Waverly LLC, USA) weighing 3–3.5 Kg were first selected for their ability to walk regularly and continuously for several minutes (10–15 min) on a motor-driven treadmill at the speed of 0.4 m/s. The cats were housed together in a 36 m<sup>2</sup> room with a 12 h light/dark cycle and had free access to food and water. Cats were implanted with electrode arrays within the hindlimb representation of both motor cortices. In addition, intra-muscular electrodes were implanted in the flexor and extensor muscles in both hindlimbs. The immediate effects of uni-cortical and bi-cortical micro-stimulation on treadmill locomotion was tested using different stimulation parameters (timing, train duration, amplitude, and site). Cats then received a contusive SCI at spinal level T10. We next evaluated the immediate effects of cortical stimulation (applied to each cortex and alternately to both cortices) on the locomotor output during the entire week following recovery of unsupported treadmill locomotion. Spontaneous treadmill locomotion was also tested biweekly throughout recovery (week 1–5), as well as functional responses to cortical stimulation and stimulation thresholds (Fig. 7). Kinematic analyses were automatically performed using DeepLabCut (Lecomte et al., 2021; Mathis et al., 2018) and manually curated to correct misdetections. Obstacle avoidance performance was tested weekly, and analyses were double blinded. At the end of the experiments, after intracardiac perfusion, the spinal cord was extracted and processed for histological assessment of the spinal contusion. All procedures followed the guidelines of the Canadian Council on Animal Care and were approved by the Comité de Déontologie de l'Expérimentation sur les Animaux (CDEA, animal ethics committee) at Université de Montréal. All animals were included in the study.

### 2.2. Surgical procedures

All surgical procedures for electrode implantation or spinal lesions were conducted under general anesthesia and aseptic conditions.

Animals were premedicated with Atravet (0.05 mg/kg), glycopyrrolate (0.01 mg/kg), and ketamine (10 mg/kg) by intramuscular administration. An endotracheal tube was then inserted to provide gaseous anesthesia (2 % isoflurane in a mixture of 95 % O<sub>2</sub> and 5 % CO<sub>2</sub>). In the first surgery, cats were implanted with intramuscular electrodes to record EMG activity from flexor and extensor hindlimb muscles on both sides, and they were also implanted with intracortical arrays to stimulate the hindlimb motor cortices during locomotion. The implanted muscles were semitendinosus (St; knee flexor and hip extensor), sartorius (Srt; hip flexor and knee extensor), vastus lateralis (VL; knee extensor), gastrocnemius lateralis and medialis (GL and GM; ankle extensors and knee flexors), as well as tibialis anterior (TA; ankle flexor). Electrodes were led subcutaneously to two 15-pinhead connectors secured to the cranium using acrylic cement. During the same surgery, a craniectomy was performed to expose the cruciate sulcus of both hemispheres and the dura was resected. The electrode array was stereotactically inserted into the posterior bank of the cruciate sulcus that contains the hindlimb representation of the motor cortex (Bretzner and Drew, 2005b; Ghosh, 1997; Nieoullon and Rispal-Padel, 1976). One electrode array was inserted so as to reach layer V of each motor cortex (Fig. S3). In the first cat, a 5-channel array (P1 Technologies, USA) was implanted into the left motor cortex and 10 polyimide-coated stainless steel microwires (diameter: 50 µm, FineWire, USA) were individually implanted into the right motor cortex. The P1 Technologies array consisted of five individual electrode shanks (stainless steel, diameter: 250 µm) and a common ground. The other two cats were implanted with 32-channel arrays consisting of 4 shanks (silicon, length: 5 mm), spaced by 400 µm, each featuring 8 iridium active sites, spaced by 200 µm (NeuroNexus, USA). The most anteromedial site was lowered at 2 mm caudal to the cruciate sulcus and 2.5–3 mm lateral to the medial line, with a 20° angle from vertical, directed caudally. Coordinates were calculated to place cortical layer V approximately midway along the active sites of the shanks (Fig. S3B). The cortex was covered with a hemostatic material (Gelfoam) and the arrays and EMG connectors were attached to the cranium with 8–10 screws and dental acrylic. Four to eight weeks after EMG and intracortical array implantation, a spinal contusion at T10 was achieved under anesthesia using a modified version of the Infinite Horizon Impactor model 0400 (Precision Systems and Instrumentations, USA) (Delivet-Mongrain et al., 2020). The impactor was mounted on the side of a spinal contention unit allowing the fixation of the T10 vertebra with clips to minimize movement during the application of the impactor tip. A force of 700 kdyne (7 N), with a 15 ms rise time, was maintained for 30 s through a 5 mm diameter flat circular tip applied on the dura. Heart rate and respiration were monitored throughout the surgeries. Twenty-four hours before each surgery, an antibiotic (Convenia, 8 mg/kg) was administered subcutaneously. Before the end of the surgery, the analgesic buprenorphine (0.01 mg/kg) was administered subcutaneously. Additionally, a fentanyl patch (25 µg/h) was sutured to the skin to alleviate pain for ~5 days. Gabapentin (10 mg bid) was also given for 3 days to alleviate pain if needed, after the implantation but not the spinal contusion surgery.

### 2.3. Behavioral assessments and analyses

Stepping patterns and skilled locomotion were assessed using the following two tasks: (1) treadmill without obstacles, and (2) treadmill with obstacles. Before the first surgery, all cats were trained to walk on a treadmill with positive reinforcement. They were not trained to avoid obstacles, but we occasionally introduced obstacles during the habituation period. During episodes of locomotion at the speed of 0.4 m/s, cats were recorded from the left and right sides with a digital video camera (120 Hz, Teledyne FLIR, USA). The kinematic analyses and the obstacle avoidance scoring were performed offline.

## 2.4. Kinematic analysis

Reflective markers were placed over the iliac crest, the greater trochanter, the lateral malleolus, the metatarsophalangeal (MTP) joint, and at the tip of the fourth toe of the left and right hindlimbs. Following data acquisition, we analyzed locomotor episodes of  $10 \pm 2$  consecutive step cycles using DeepLabCut (Lecomte et al., 2021; Mathis et al., 2018) and manually curated to correct misdetections. A step cycle represents the time between two successive contacts of the same foot on the treadmill, beginning and ending with a foot strike. Hindlimbs are referred to as contralateral or ipsilateral to the stimulated cortex. The contralateral hindlimb is located on the opposite side of the stimulated cortex and the ipsilateral hindlimb is on the same side.

The following different kinematic parameters (indicated in italics) were used to evaluate the stepping abilities:

The *step height* represented the maximum height (cm) of the foot during the swing phase. The *flexion velocity* corresponded to the maximum vertical speed (cm/s) reached by the foot during the swing phase. The *toe trajectory* represented the trajectory of the hindlimb's toe (tip of the 4th toe) during the step cycle. The *foot drag* was quantified as the time (expressed as a percentage of the swing phase) where the dorsal part of the distal phalanx of a given hindpaw dragged over the treadmill belt. The *lift* was the moment at which the foot took off from the treadmill belt and the *contact* was the moment at which it contacted the belt. In order to normalize a step cycle, we used the contact of the hindlimb ipsilateral to the stimulated cortex as a reference. The *lift phase* corresponded to the moment at which the lift of the contralateral hindlimb occurred in a normalized step cycle. The *lift phase variability* was the standard deviation of the lift phase inside a locomotor episode ( $10 \pm 2$  step cycles). The *contact phase* corresponded to the moment at which the contact of the contralateral hindlimb occurred in a normalized step cycle. The *stimulation onset phase* corresponded to the moment at which the stimulation train began during a normalized step cycle. The *stimulation precision* indicated the % of all stimulations for which stimulation onset phase fell into an interval of the step cycle (expected stimulation time window) eliciting an optimal motor response i.e. the highest step height increase in the intact state and the maximal reduction of dragging after SCI. Stimulation at the lift of the contralateral hindlimb produced the highest response, but an optimal response was observed with stimulation delivered within a time window, around the lift, corresponding to 20 % of the step cycle. This interval included the lift of the contralateral hindlimb. The *foot position at contact* was the distance (cm) between the toe and the hip (vertical projection of the hip's position) at the hindlimb's contact. This value indicated the extent of forward movements during a locomotor episode. The *step cycle duration* represented the time (s) between two consecutive contacts of the same foot on the treadmill, whereas *swing duration* referred to the time (s) between toe-off and foot contact. The *stance duration* referred to the time between foot contact and toe-off. The *trajectory modulation* comprised the time series representing the average effect of a given stimulation condition on the swing trajectory. They were defined as the difference between spontaneous trajectories and modulated trajectories, in polar coordinates. The center of the polar coordinate system was set at the center of the segment connecting the points where the foot takes off the ground and strikes the ground. The *centroidal axes of toe trajectories* are vectors indicating the centroid (in polar coordinates) of trajectory modulations, as depicted in Fig. 4E. Multivariate analysis consisted of a PCA dimensionality reduction of each trajectory modulation series into the 2D space of the two principal components. Each projected point represents the average modulation obtained with a given stimulation condition.

## 2.5. Obstacle avoidance analysis

Following a paradigm established by Drew (1993), an obstacle (height: 5 cm; anteroposterior width: 5 cm; mediolateral width: 35 cm) was placed on the treadmill belt. Five-minute videos were captured

weekly and analyzed in double blind to evaluate the ability to step over the obstacle without touching it in the intact state and after spinal contusion.

## 2.6. Phase-coherent ICMS during locomotion

Biphasic (cathodic first) 330 Hz stimulations were delivered with a Tucker-Davis Technologies (USA) stimulator during treadmill locomotion. A simple EMG pattern recognition algorithm was used to detect the gait phases (Bonizzato and Martinez, 2021). EMG signals were digitized at 6 kHz (anti-aliasing filter at 45 %) and filtered online (bandpass, 70–700 Hz) using a real-time BioAmp processor (Tucker-Davis Technologies, USA). Each time the filtered and rectified signal from a selected muscle (gastrocnemius medialis ipsilateral to the stimulated cortex) reached a manually selected threshold, a gait synchronization event was detected, indicating the onset of muscle activity. For each detection, a refractory period of 700 ms was imposed to prevent eliciting triggers within a single EMG burst. Synchronization triggered the delivery of a phasic stimulation to a selected electrode in the array (100 ms train, 330 Hz frequency, biphasic, cathodic first, 200  $\mu$ s/phase, and 50  $\mu$ s phase interval). For intact cats, 1–4 electrode sites per cortex were chosen for recordings after visually determining that they elicited different types of movements. This initial survey was performed by rapidly switching between available active sites while the cat was walking, until a putative visually different movement was obtained. The selected active site was then studied through more extensive kinematics recordings, including five stimulation amplitudes. After contusion, the same survey was performed but only one type of flexion movement was reported. 1–3 electrode sites per cortex were chosen for their ability to produce a flexion movement and attempting to represent a variety of spatial location over the electrode array.

### 2.6.1. Phase-coherent uni-cortical stimulation

In intact cats and SCI cats, we tested the effects of varying stimulation parameters on the evoked locomotor output. During locomotor episodes, uni-cortical stimulation was delivered with one parameter being modulated while the others remained constant. Uni-cortical stimulation was defined as stimulation that was delivered to only one motor cortex during a locomotor episode. The modulated parameters were the timing, the train duration, the amplitude, and the site of stimulation. When the parameters were kept constant, we used: a sub-maximal amplitude (high amplitude), a 200 ms delay after synchronization event detection (corresponding to the contralateral hindlimb's lift), and a 100 ms train duration. Using these constant parameters during locomotion, each electrode site of each array was tested for its ability to influence the contralateral hindlimb's trajectory, and for the qualitative nature of that influence, effectively providing a map of the motor cortical representation accessible for modulation of each hindlimb in each cat (Fig. S3). For the study of timing, train duration, and amplitude, diverse stimulation channels within each cortical array were selected among those with the lowest current threshold for evoking movement.

**2.6.1.1. Timing.** To assess the effects of stimulation delivered at different phases of the step cycle, multiple delays between the detection of ipsilateral or contralateral gastrocnemius medialis activity onset and the delivery of the stimulation (0, 100, 200, 300 and 400 ms for each muscle) were used. Each delay corresponded to separate timings in the gait cycle enabling covering of the entire step cycle. Each delay was tested randomly. Every delay (in ms) between the synchronization event and the onset of stimulation was the same, but the exact normalized phase of the step cycle at which the onset of stimulation occurred varied. The data was linearly interpolated using Interp1 (MATLAB 2019b) and was averaged across all tested sites and all cats.



**2.6.1.2. Train duration.** Both before and after SCI, the effect of train duration on the evoked motor response was tested using four different stimulation train durations: 50, 100, 150, and 200 ms.

**2.6.1.3. Amplitude.** The stimulation amplitude was modulated within a “functional range” of amplitudes. During ongoing locomotion, we stimulated with increasing amplitudes to find the threshold (i.e. the smallest amplitude evoking a visible response; intact: 10–75  $\mu$ A, post-SCI: 50–300  $\mu$ A), which corresponded to the beginning of the range. We then continued to increase the amplitude until the maximum comfortable value was reached (intact: 30–250  $\mu$ A, post-SCI: 100–500  $\mu$ A). The range was divided into five amplitudes (threshold, low, medium, high, and maximum) for intact cats and three amplitudes (threshold, medium, and maximum) for SCI cats. The medium value indicates the average between the threshold value and the maximum value (50 % of the range). The low and high values represent 25 % and 75 % of the functional range, respectively. The different amplitudes were randomly tested for every stimulation site.

### 2.6.2. Phase-coherent bi-cortical stimulation

We also tested whether stimulation applied alternately to the left and right motor cortex during walking could bilaterally modulate hindlimb locomotion.

The stimulation was delivered to both cortical hemispheres alternately and phase-coherently during treadmill locomotion (delay: 200 ms after synchronization event detection, train duration: 100 ms). The stimulus amplitude applied to each cortex was independently selected and we tested all combinations (a full 2D matrix of stimulation amplitude options, left vs right cortex:  $4 \times 4$  for intact cats and  $3 \times 3$  for SCI cats). In intact cats, four different conditions were used: off (no stimulation), threshold, medium, and maximum. In SCI cats, only three conditions were tested: off (no stimulation), medium, and maximum.

### 2.7. Evaluation of the lesion size

At the end of the experiments, the animals were deeply anesthetized with ketamine (Ketaset; 10 mg/kg; intramuscular) and administered a lethal dose of pentobarbital (Euthanyl; 120 mg/kg; intravenous). The animals were perfused transcardially with a solution of 0.2 % heparin in 0.1 M phosphate-buffered saline (PBS; pH 7.4), followed by 4 % paraformaldehyde (PFA) in 0.1 M PBS (pH 7.4). The brain and the spinal cord were extracted and postfixed for 24 h in a solution of 16 % PFA in 0.1 M PBS. The tissue was then cryoprotected in a solution of 30 % sucrose in 0.1 M PBS. The spinal cord was frozen, and 40  $\mu$ m thick coronal sections centered on the spinal lesion were taken for histological examination. Every third section was mounted on slides and stained with Luxol fast blue (0.1 %, Sigma, USA S3382) to visualize myelin in the spinal white matter and cresyl violet (0.5 %, Alfa Aesar, USA J64318) to visualize cell bodies in the spinal gray matter. Bright-field microscopy images were taken at 4X (Olympus BX63) and analyzed using cellSens software (Olympus, Japan). Lesion extent was quantified by evaluation of the percentage of damaged and intact tissue of the cord observed in the coronal plane. Each image area was assigned to one of three categories [cavity, damage, intact], and the number of pixels belonging to each category was counted.

### 2.8. Quantification and statistical analyses

All data are presented as the mean values  $\pm$  SEM. All statistical analyses were performed using GraphPad Prism 6 or MATLAB software. The normal distribution of the data was assessed using the Anderson-Darling test. We first performed one-way repeated measures ANOVAs. The Bonferroni test was used as a post-hoc for multiple comparisons. When multiple comparisons were conducted, the Holm-Bonferroni method was used to re-establish the level of significance and control

for false positives. The tests were one-sided because our hypotheses were strictly defined toward the direction of motor improvement. The statistical significance threshold was set at  $P = 0.05$ .

## 3. Results

We designed a neuroprosthetic platform whereby ongoing locomotor phases were monitored through real-time online processing of electromyographic (EMG) activity from hindlimb muscles (Fig. 1). Hindlimb contacts with the ground during gait (“foot-strikes”) were detected by pattern recognition of gastrocnemius muscle activity. ICMS was triggered at a fixed delay following foot-strikes, corresponding to the expected lift of the hindlimb contralateral to the stimulated cortex. Before and after a spinal cord contusion, we first characterized the effects of multiple stimulation parameters on kinematics, including timing, stimulus duration, amplitude, and site of stimulation. We explored ICMS controllability over a repertoire of varied hindlimb movements. Before and after a spinal cord contusion we also tested whether bi-cortical ICMS could be used to control bilateral gait performance by enforcing alternated patterns of stimulation, coherent with each hindlimb’s movement. After SCI, we determined what stimulation parameters maximally alleviated foot drop. We found that the re-emergence of cortical neuroprosthetic control of movement and spontaneous weight-supporting locomotion occurred concomitantly in all cats.

### 3.1. Phase-coherent ICMS modulated contralateral hindlimb kinematics in healthy cats

The modulation of hindlimb motor output enabled by ICMS was investigated in  $n = 3$  intact cats. During treadmill walking, ICMS was delivered through an electrode selected from an array implanted in the left or right hindlimb motor cortex (Fig. 2A). Using EMG pattern recognition, stimulation onset phase resided within the expected time window for optimal motor response, which corresponded to 20 % of the step cycle encompassing the lift of the contralateral hindlimb, in 83.4 % of cases (stimulation precision, Fig. S1A). Changes in hindlimb trajectory and locomotion were assessed while varying either the timing,

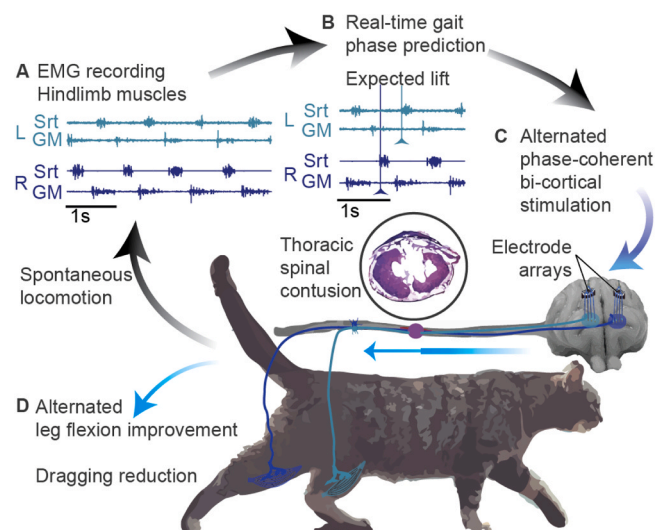


**Fig. 1.** Bi-cortical neuroprosthesis design. (A) During treadmill locomotion, electromyographic activity was recorded from flexor and extensor muscles from both hindlimbs. (B) EMG activity was analyzed in real-time to predict the occurrence of each hindlimb’s foot lift. (C) Lift prediction triggered ICMS delivery to hindlimb motor cortices. (D) ICMS applied to the right motor cortex enhanced leg flexion of the left hindlimb and conversely, modulating bilateral locomotor output. L: left, R: right, Srt: sartorius, GM: gastrocnemius medialis, and s: seconds.

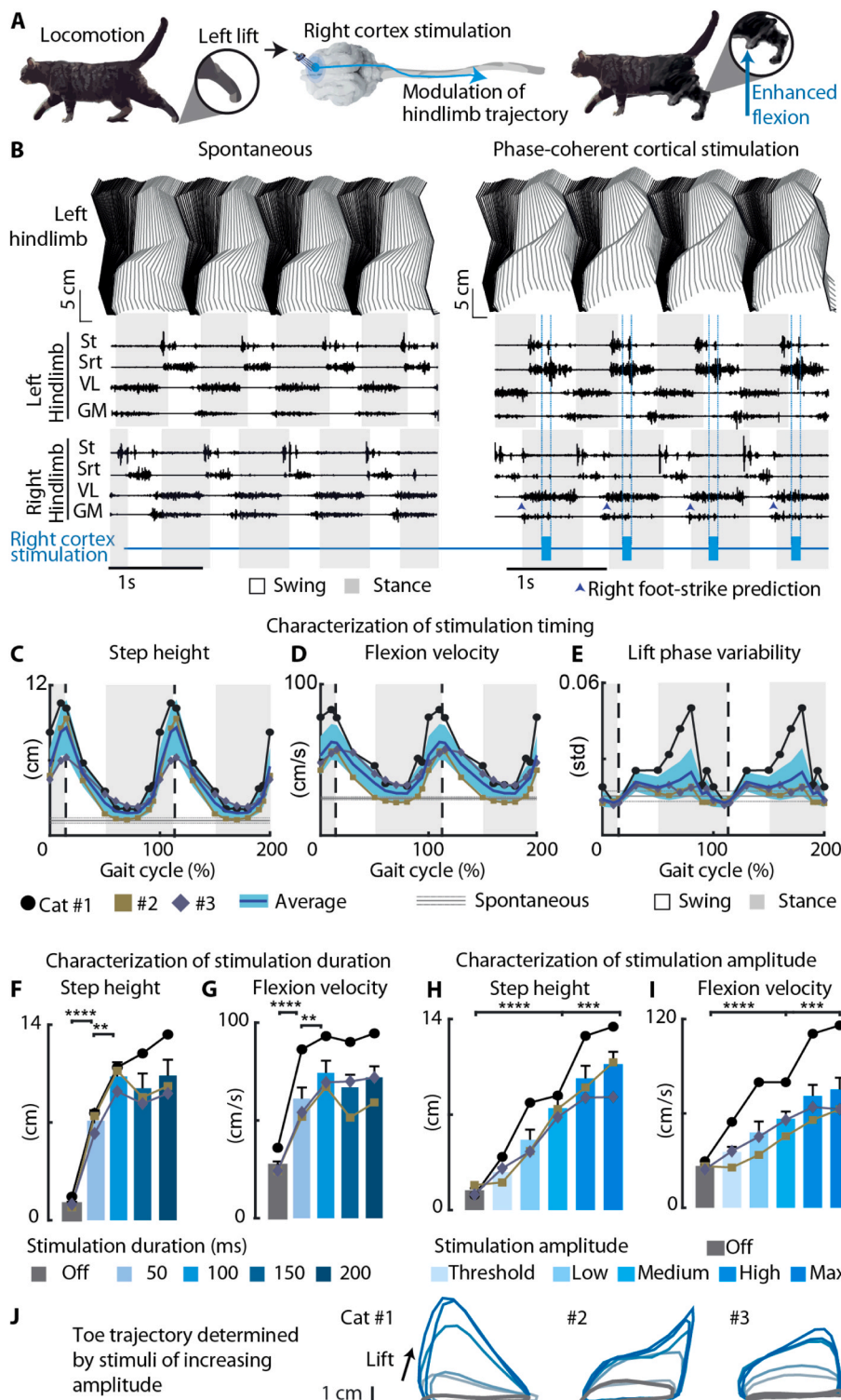


**Fig. 2.** Uni-cortical stimulation modulated contralateral hindlimb kinematics in intact cats. (A) Schematic representation of uni-cortical neurostimulation: right cortex stimulation modulated left hindlimb flexion through descending projections. (B) Stick diagram and EMG activity during spontaneous locomotion and phase-coherent ICMS delivered to the right cortex. Changes in (C) step height, (D) flexion velocity, and (E) lift variability ( $n = 17$  sites, 3 cats) as a function of stimulus delivery timing along the gait cycle. Changes in (F) step height and (G) flexion velocity ( $n = 16$  sites, 3 cats) as a function of train duration. Increasing ICMS amplitude linearly modulated (H) step height, (I) flexion velocity ( $n = 17$  sites, 3 cats), and (J) toe trajectories. The dashed lines in panels C–E indicate the percentage of the step cycle at which the measures of ICMS-evoked movements were performed in panels F–J.  $p$ : \*  $< 0.05$ ; \*\*  $< 0.01$ ; \*\*\*  $< 0.001$ ; \*\*\*\*  $< 0.0001$ . St: semitendinosus, Srt: sartorius, VL: vastus lateralis, and GM: gastrocnemius medialis.

duration, or amplitude of the stimulation.

Stimulus timing played a critical role in neuromodulation efficacy. When delivered at the beginning of the contralateral hindlimb swing, ICMS produced an enhanced contralateral hindlimb flexion in comparison to spontaneous walking (Fig. 2B). The largest changes in step height ( $p < 0.0001$ , up to an average of  $+575 \pm 185$  % of spontaneous walking: peak 8.04 cm vs 1.19 cm on average) and flexion velocity ( $p < 0.0001$ , up to  $+141 \pm 47$  % of spontaneous walking: peak 59.3 cm/s vs 24.6 cm/s on average) were obtained when ICMS was

delivered between the contralateral hindlimb lift preparation (late stance) and execution (early swing) (Fig. 2C–D). Conversely, ICMS delivered during the contralateral hindlimb's stance phase did not modulate step height and flexion velocity in comparison to spontaneous locomotion ( $p > 0.05$ ). ICMS delivered in the middle of the contralateral hindlimb's stance phase disrupted locomotion (Fig. 2E) and increased the lift phase variability ( $p < 0.05$ , up to  $+62 \pm 61$  %: peak 0.022 sd. vs 0.015 sd. on average). ICMS had no effect on the ipsilateral hindlimb's kinematics, even when delivered during its swing phase (Fig. S2A–B).

We defined ICMS to be “phase-coherent” with locomotion when delivered in phase with the contralateral hindlimb lift preparation.

We then evaluated the impact of phase-coherent ICMS duration on hindlimb flexion. The largest increase in step height ( $p < 0.0001$ ,  $+766 \pm 85$  % of spontaneous walking: peak 10.29 cm vs 1.19 cm on average) and flexion velocity ( $p < 0.0001$ ,  $+173 \pm 23$  % of spontaneous walking: peak 74.4 cm/s vs 27.2 cm/s on average) were obtained with a 100 ms stimulation duration (Fig. 2F–G). Kinematic modulation plateaued for longer durations. A 100 ms duration was considered optimal and was

consequently used in all experiments.

We also examined the effects of varying phase-coherent ICMS amplitude on hindlimb flexion, revealing a high-fidelity proportional control of motor output. Stimulation amplitude featured precise control over contralateral step height and toe trajectories (Fig. 2H–J) but had no impact on ipsilateral hindlimb flexion (Fig. S2C–D). Contralateral step height ( $p < 0.0001$ , up to  $+733 \pm 62$  % of spontaneous walking: peak 10.70 cm vs 1.45 cm on average, fit  $r^2$ :  $90 \pm 2$  %) and flexion velocity ( $p < 0.0001$ , up to  $+183 \pm 28$  %: peak 75.2 cm/s vs 26.5 cm/s on

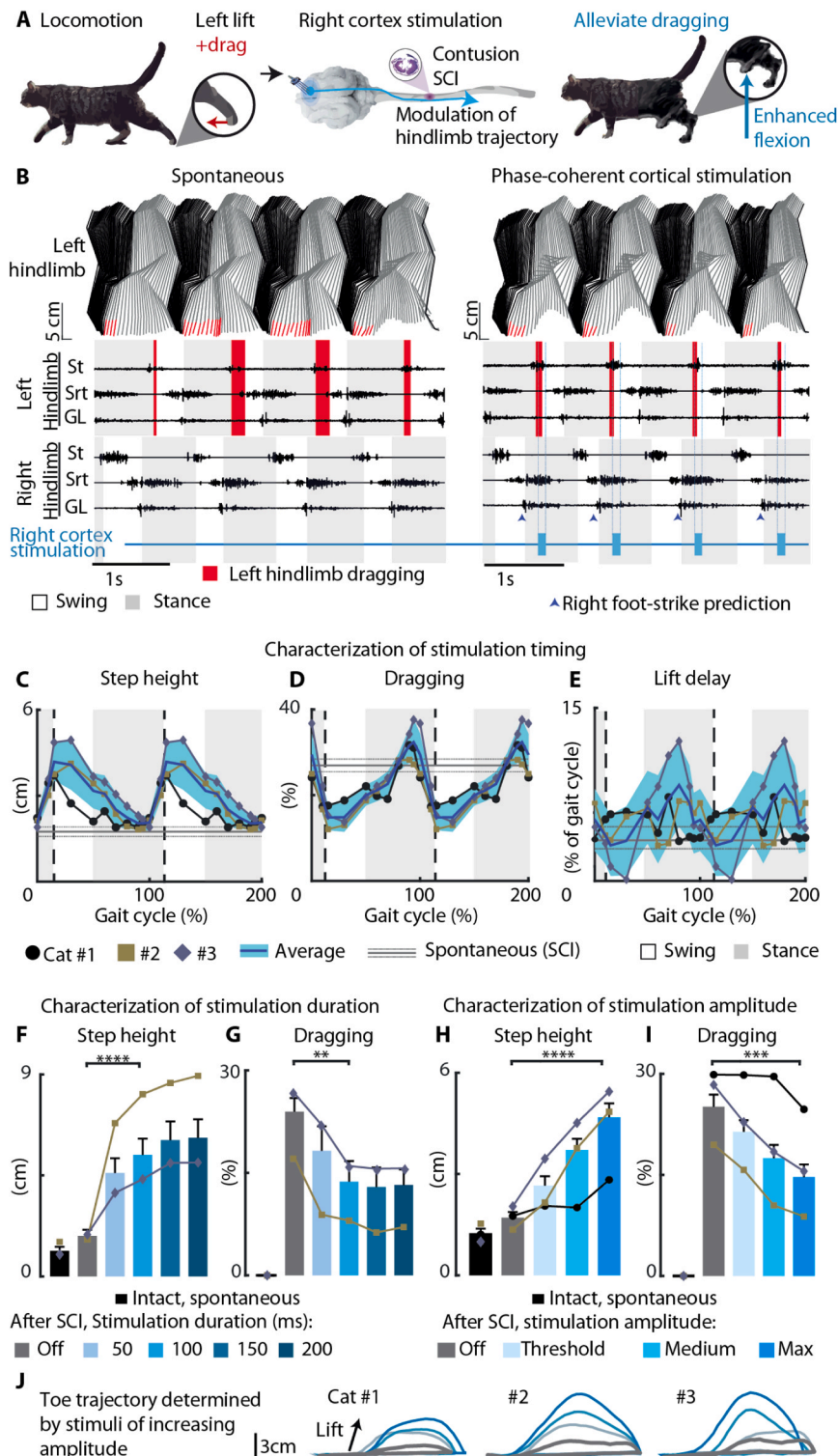


**Fig. 3.** Uni-cortical stimulation alleviated contralateral hindlimb deficits after SCI. (A) Schematic representation of uni-cortical neurostimulation following thoracic spinal cord contusion. ICMS modulated contralateral hindlimb locomotion through spared descending nerve fibers. (B) Stick diagram and EMG activity during spontaneous locomotion and with phase-coherent ICMS delivered to the right cortex. When applied during swing execution, ICMS enhanced (C) step height and reduced (D) dragging. When applied during mid-stance, ICMS modified the (E) lift delay of the contralateral hindlimb ( $n = 15$  sites, 3 cats). The train duration modulated the (F) step height, and reduced (G) dragging of the contralateral hindlimb ( $n = 7$  sites, 2 cats). The stimulation amplitude linearly increased the (H) step height, decreased (I) dragging ( $n = 15$  sites, 3 cats), and modulated the (J) toe trajectories. The dashed lines in panels C–E indicate the percentage of the step cycle at which the measures of ICMS-evoked movements were performed in panels F–J.  $p$ : \*  $< 0.05$ ; \*\*  $< 0.01$ ; \*\*\*  $< 0.001$ ; \*\*\*\*  $< 0.0001$ . St: semitendinosus, Srt: sartorius, and GL: gastrocnemius lateralis.



average of spontaneous walking, fit  $r^2$ :  $85 \pm 3$  %) modulated linearly with increasing stimulation amplitudes (Fig. 2H–I). The average threshold amplitude was  $29 \mu\text{A}$ , with a standard deviation (S.D.) of  $16 \mu\text{A}$ , and the maximum was  $136 \mu\text{A}$  (S.D.  $61 \mu\text{A}$ ). The functional range of stimulation amplitudes spanned 2.3x to 10x threshold values.

### 3.2. Phase-coherent ICMS modulated contralateral hindlimb kinematics after SCI

Thoracic spinal cord contusion produced complete acute bilateral hindlimb paralysis. Two to three weeks after SCI, all  $n = 3$  cats exhibited weight-supported bilateral hindlimb locomotion, despite severe dragging (Fig. 3A–B). We tested the immediate effects of phase-coherent ICMS during treadmill walking. Timely delivery of the stimulation to selected electrodes in the right or left motor cortex was achieved with 88.2 % precision (Fig. S1C).

Stimulus timing played a critical role in neuromodulation efficacy after SCI. Phase-coherent ICMS successfully enhanced contralateral hindlimb flexion, which, in turn, alleviated dragging in all tested animals (Fig. 3B). An increase in step height ( $p < 0.0001$ , up to  $+140 \pm 37$  % of spontaneous walking: peak  $4.18 \text{ cm}$  vs  $1.75 \text{ cm}$  on average; Fig. 3C) and reduction of dragging ( $p < 0.001$ , up to  $-45 \pm 11$  % of spontaneous walking: lower bound  $14.8$  % vs  $26.9$  % on average; Fig. 3D) were maximal when stimulation was delivered during contralateral swing execution. Conversely, stimulation delivered during contralateral swing preparation did not significantly increase step height ( $p > 0.05$ ,  $+19 \pm 16$  % of spontaneous walking post-SCI:  $2.04 \text{ cm}$  vs  $1.75 \text{ cm}$  on average, Fig. 3C) and was associated with a non-significant increase in dragging ( $p > 0.05$ , up to  $+20 \pm 20$  % of spontaneous walking: peak  $32.37$  % vs  $26.94$  % on average, Fig. 3D). When stimulation was delivered in the middle of the contralateral stance phase, it disrupted the step cycle by delaying the beginning of the lift phase ( $p < 0.05$ , up to  $+13 \pm 10$  % of spontaneous walking: peak  $0.128 \text{ S.D.}$  vs  $0.113 \text{ S.D.}$  on average, Fig. 3E). As observed in intact cats, ICMS did not affect ipsilateral hindlimb step height and flexion velocity, regardless of the stimulation timing delivery in the locomotor cycle (Fig. S2E–F). Hence, in SCI cats, we defined stimulation as “phase-coherent” with locomotion when delivered during the execution phase of the contralateral hindlimb lift.

We then evaluated the effects of phase-coherent ICMS duration on hindlimb flexion. Consistently with the results obtained in the intact state, a 100 ms stimulation train produced a significant increase in step height ( $p < 0.0001$ ,  $+375 \pm 63$  % of spontaneous walking:  $5.41 \text{ cm}$  vs  $1.14 \text{ cm}$  on average, Fig. 3F), which, in turn, decreased dragging ( $p < 0.01$ ,  $-43 \pm 13$  % of spontaneous walking:  $13.72$  % vs  $23.95$  % on average, Fig. 3G). Since further increasing the stimulus duration only generated minimal gains in movement modulation, stimulus duration was maintained at 100 ms in all subsequent experiments.

We finally examined the effects of varying phase-coherent ICMS amplitude on hindlimb flexion after SCI (Fig. 3H–J). As observed in the intact state, ICMS amplitude modulated contralateral leg trajectory (Fig. 3J), with no impact on ipsilateral hindlimb flexion (Fig. S2G–H). Contralateral step height ( $p < 0.0001$ , up to  $+274 \pm 33$  % of spontaneous walking: peak  $4.68 \text{ cm}$  vs  $1.25 \text{ cm}$  on average, fit  $r^2$ :  $76 \pm 7$  %, Fig. 3H), and dragging reduction ( $p < 0.0001$ , up to  $-42 \pm 7$  % of spontaneous walking: lower bound  $16.7$  % vs  $25.1$  % on average, fit  $r^2$ :  $68 \pm 7$  %, Fig. 3I) modulated linearly with increasing stimulation amplitudes. As all cats displayed some asymmetries in foot clearance capacity (measured as step height, Fig. S6F–G), modulating the intensity of cortical stimuli allowed tuning step height symmetry. At any given stimulation condition, increasing stimulation amplitude in the left cortex would increase step height in the right hindlimb, and vice versa (Fig. S6F).

After SCI, the average threshold amplitude was  $105 \mu\text{A}$ , with a S.D. of  $81 \mu\text{A}$ , and the maximum was  $295 \mu\text{A}$  (S.D.  $102 \mu\text{A}$ ). The functional range of stimulation amplitudes spanned 1.6x to 6x threshold values.

### 3.3. Phase-coherent ICMS produced diverse movement synergies in intact cats that were lost after SCI

ICMS produced a variety of motor outputs in intact cats. When selecting different electrode sites within the hindlimb motor cortex representation (Fig. S3), we were able to impose qualitative changes to hindlimb trajectories during hindlimb swing. Six distinct motor programs were recruited across intact animals, with 2–4 programs expressed for selected sites per cat, and the associated gait trajectories were characterized under increasing stimulation amplitudes (Fig. 4A–B, Fig. S4, Movie S1). Each movement remained qualitatively similar with varying stimulation amplitudes within the same electrode, while varying in the extent of trajectory modulation (Fig. 4A). Switching between different stimulation electrodes, we obtained trajectory modulations consisting of backward flexions, abductions, forward flexions, qualitatively different upward flexions, including ones appearing ‘natural’ (i.e., a smooth, curved progression of the limb up and forward), as well as some associated with a co-contraction of flexor and extensor muscles (Fig. 4B). There was a variability in the distribution of evoked movements across intact cats (Fig. 4B, Fig. S4). In cat #3, we also identified a swing-stop control (Fig. S5A), whereby stimulation delivery shortened the swing movement, resulting in curtailment of the step (Fig. S5B–C). We repeated the same characterization after SCI and found that this evoked movement diversity was absent. Across all cats, stimulation resulted in upward-directed modulation of hindlimb flexion, for all sites and stimulation amplitudes (Fig. 4C–D).

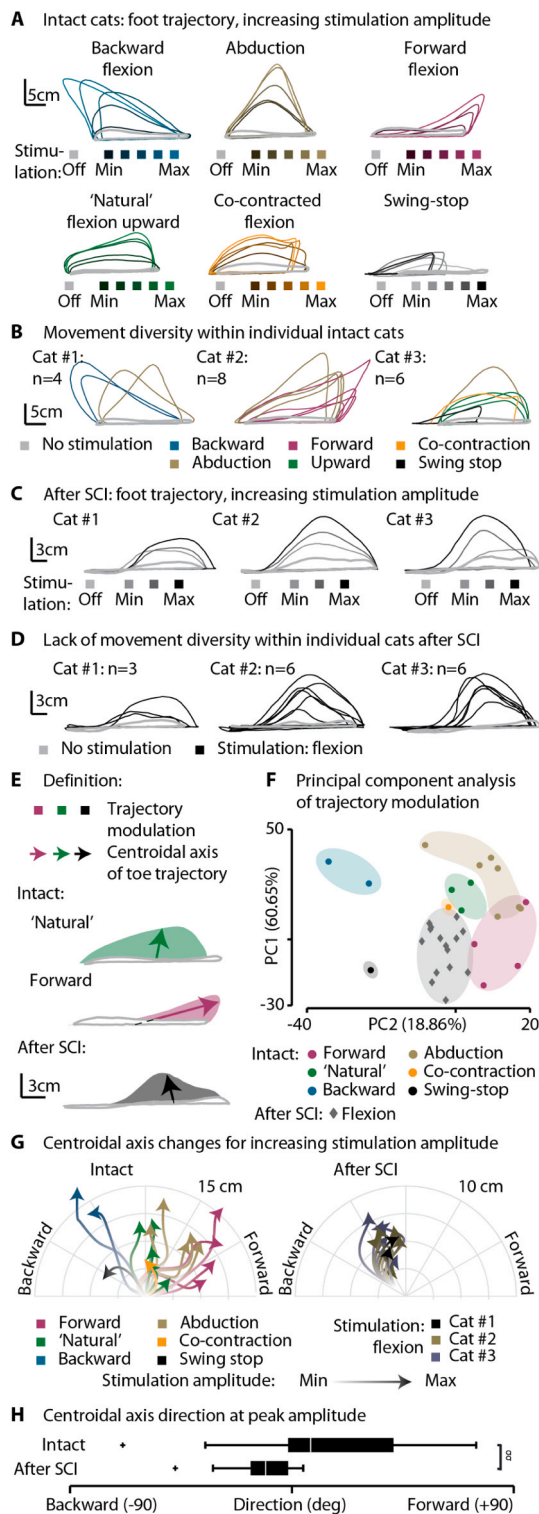
We performed an analysis of movement trajectories by (1) comparing the main direction of toe trajectory modulation during swing (‘centroidal axis of toe trajectory’) (Figs. 4E) and (2) performing multivariate analysis (principal component analysis, PCA) of toe trajectories (Fig. 4F) across all motor programs. PCA grouped the identified motor programs in separate zones of the principal component space, with movements evoked in intact cats scattered throughout the PC space, and the evoked movements were different across cats (Fig. 4B, S4D). In contrast, all movements evoked after SCI were concentrated in only one area, and equally distributed across cats (Fig. 4C, S4D).

Analysis of the trajectory in intact cats displayed a large repertoire of directional swing movement modulations. After SCI, all modulations were pointed within a restrained portion of the polar diagram (Fig. 4G–H,  $p < 0.01$ : two-sample two-sided F-test for equal variances).

### 3.4. Phase-coherent bi-cortical stimulation bilaterally modulated hindlimb trajectories in intact and SCI cats

Since phase-coherent ICMS delivered to one cortex modulated contralateral hindlimb movements, we hypothesized that alternately stimulating both motor cortices would allow bilateral control of foot trajectories. Using EMG pattern recognition, delivery of the stimulation was triggered with a 97.6 % and 98.1 % timing precision in intact and SCI cats, respectively (Fig. S1B–D). Before and after contusive SCI, phase-coherent ICMS (100 ms) was delivered alternately to the left and right motor cortex during treadmill walking in  $n = 3$  cats (Figs. 5A and 6A). Delivery of bi-cortical stimulation induced an alternated increase of hindlimb flexion in intact cats (Fig. 5B, Movie S2). After SCI, phase-coherent bi-cortical stimulation immediately improved the bilateral locomotor pattern, enhancing hindlimb flexion, which, in turn, alleviated dragging deficits (Fig. 6B, Movie S3). The beneficial effects of ICMS disappeared when the stimulation was discontinued.

Next, we investigated the extent to which the specific cortical control of contralateral hindlimb movements is independent from interactions with the activated homologous cortex. This analysis was performed to ensure that, during alternated bi-cortical stimulation, ICMS delivered to the homologous cortex did not interfere with ICMS delivered to the contralateral cortex. Thus, we combined the stimulation delivered to the right and left motor cortex, independently selecting the stimulus amplitude on each cortex and testing all combinations (a 2D



(caption on next column)

**Fig. 4.** Uni-cortical stimulation triggered a variety of motor synergies in intact cats and a single stereotyped lift movement after SCI. (A) Six different movements evoked by varying stimulation electrodes across three intact cats. For each stimulation electrode, superimposed trajectories were color-coded for the tested range of stimulation amplitudes. (B) The peak modulations of each tested electrode were superimposed for each cat. (C) Movements evoked by cortical stimulation across three SCI cats. For each stimulation electrode, superimposed trajectories were color-coded for the tested range of stimulation amplitudes. (D) The peak modulations of each tested electrode were superimposed for each cat. (E) Schematic description of the trajectory modulation assessments (difference in foot trajectory with and without stimulation) and centroidal axis of toe trajectory. (F) Principal component analysis of trajectory modulations. Each dot represents a trajectory from panels B and D. The data were color-coded by visual qualification of evoked movements. (G) Centroidal axis change for intact and SCI cats. The arrows follow increasing stimulation amplitudes. (H) Distribution of centroidal axis of toe trajectory under peak stimulation amplitudes.  $\sigma$ :  $p < 0.01$ , the symbol  $\sigma$  indicates a statistical test of the distributions' variances. PC: principal component.

hindlimb movements (Fig. S6A-B).

After SCI, increasing stimulation amplitudes produced a linear increase in contralateral hindlimb step height ( $p < 0.01$ , up to +196 % ~ +216 % of spontaneous walking post-SCI, fit  $r^2$ :  $84 \pm 5$  %, Fig. 6C) and flexion velocity ( $p < 0.05$ , up to +70 % ~ +78 % of spontaneous walking post-SCI, fit  $r^2$ :  $75 \pm 5$  %, Fig. 6D), which, in turn, produced a linear decrease in dragging ( $p < 0.001$ , up to -42 % ~ -53 % of spontaneous walking post-SCI, fit  $r^2$ :  $76 \pm 6$  %, Fig. 6E). The specific effect of cortical stimulation on contralateral hindlimb movements was independent from the level of stimulation of the homologous cortex (Fig. S6C-E).

### 3.5. The return of locomotion after SCI was correlated with descending drive recovery

Contusive SCI are characterized by the interruption of variable pathways and pronounced secondary damage, including cavity formation (Delivet-Mongrain et al., 2020). In this study, the spinal lesions exhibited central cavitations and surrounding intact tissue that contained residual descending motor pathways, including pyramidal and non-pyramidal tracts (Fig. S7A, D, and G).

The three injury profiles were associated with distinct timelines of locomotor recovery (Fig. 7A). Cat #2 first recovered weight-supported treadmill locomotion 1.5 weeks after SCI and displayed moderate (>50 %) obstacle avoidance performance by week 2 (Fig. 7A, S7E). Cat #1 was first able to walk unsupported at week 2, with low (<50 %) obstacle avoidance performance (Fig. S7B). Cat #3 also recovered weight-supported locomotion at week 2 but exhibited severe dragging deficits (>50 %) and inability to avoid obstacles (<5 %), that persisted for half a week (Fig. S7H). Consistent with higher injury lateralization towards the right of the spinal cord, the left hindlimb performance on the obstacle avoidance task was almost two-fold improved over the right one (Fig. S7H). Over the course of 5 weeks after SCI, all  $n = 3$  cats partially recovered both toe clearance during treadmill locomotion and obstacle avoidance capacity.

The three injury profiles were also associated with distinct timelines of stimulation output re-expression (Fig. 7A). Cat #2 first re-expressed cortically evoked hindlimb movements at 1.5 weeks (left hindlimb) and 2 weeks (right hindlimb) after SCI and displayed lower ICMS thresholds (<100  $\mu$ A) by week 2 and 3, respectively (Fig. 7A, S7F). Cat #1 first expressed cortical modulation of gait at week 2, with high (>250  $\mu$ A) ICMS thresholds (Fig. S7C). Cat #3 also started responding to cortical stimulation at week 2 on the left side, with high ICMS thresholds (>250  $\mu$ A), which rapidly decreased in 3 days (Fig. S7I). Again, consistent with its SCI profile, the right hindlimb responses of cat #3 to stimulation and the threshold curves of the contralateral cortex were time-shifted by 3 days. All  $n = 3$  cats re-expressed increasingly stronger

combination of stimulation amplitude options:  $4 \times 4$  for intact cats and  $3 \times 3$  for SCI cats. In intact cats, the contralateral step height ( $p < 0.01$ , up to +528 % ~ +813 % of spontaneous walking, fit  $r^2$ :  $89 \pm 1$  %, Fig. 5C) and flexion velocity ( $p < 0.01$ , up to +132 % ~ 187 % of spontaneous walking, fit  $r^2$ :  $85 \pm 3$  %, Fig. 5D) modulated linearly with increasing amplitudes. Stimulation of the homologous cortex did not interfere with the specific cortical stimulation effects on contralateral



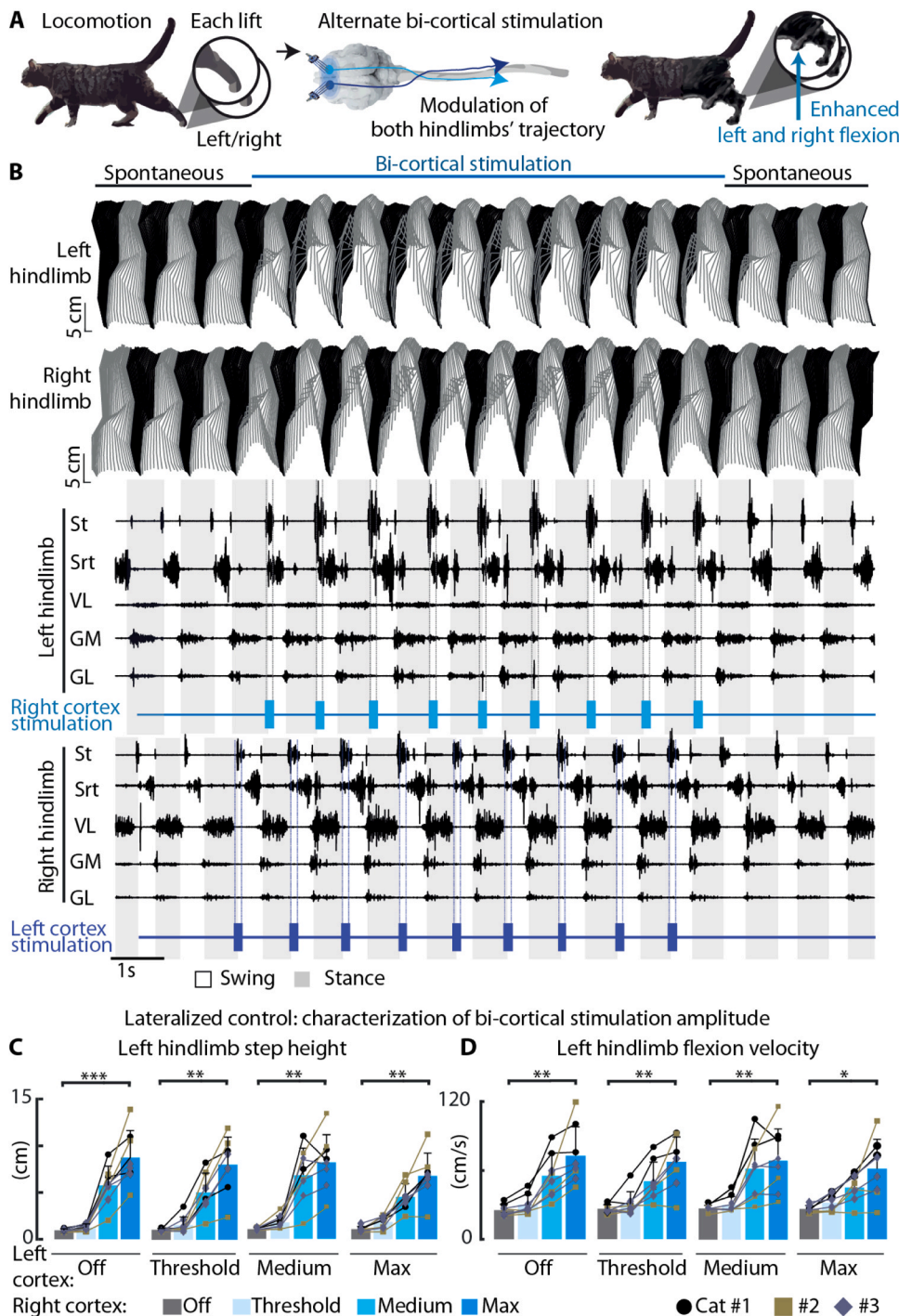


**Fig. 5.** Phase-coherent bi-cortical stimulation modulated bilateral gait kinematics in intact cats. (A) Schematic representation of bi-cortical neurostimulation. Both cortices were stimulated alternately and in phase coherence with locomotion. (B) Stick diagram and EMG activity during spontaneous walking with or without bi-cortical stimulation. During bi-cortical stimulation, the (C) left hindlimb step height and (D) left hindlimb flexion velocity linearly modulated with increasing ICMS amplitude applied to the right cortex, independently of the stimulation amplitude delivered to the homologous cortex.  $p: * < 0.05$ ;  $** < 0.01$ ;  $*** < 0.001$ . St: semitendinosus, Srt: sartorius, VL: vastus lateralis, GM: gastrocnemius medialis, and GL: gastrocnemius lateralis.

cortically-controlled gait modulation, with ICMS thresholds continuously decreasing over the course of 5 weeks after SCI (Fig. S7). The lateralization of stimulation capacity was coherent with asymmetric injury profiles and in line with the lateralization of motor deficits (Fig. 7B-C): cats displaying a right-dominant injury profile were prone to right-dominant locomotor deficits and display lesser excitability of right hindlimb responses by cortical stimulation in the early recovery timeline (week 3).

(A) Top: Cats recovered overground walking 1.5–2 weeks after SCI and were able to clear > 50 % obstacles on week 2–4 after SCI. Bottom: The first responses to cortical stimulation emerged 1.5–2 weeks after SCI and evolved into strong leg flexions (>5 cm) 2.5–3.5 weeks after SCI. The time-course of locomotor recovery of each cat correlates with the

timeline of expression of cortical stimulation capacity. (B) Asymmetries in contusive lesion outcomes (spared tissue) relate to asymmetries in locomotor capacity (obstacle avoidance and dragging). (C) Asymmetries in contusive lesion outcomes also relate to differential stimulation capacities across the two cortical hemispheres (stimulation thresholds and capacity to modulate step height).

#### 4. Discussion

We developed a bi-cortical neuroprosthesis to alleviate the severe bilateral locomotor deficits produced by contusive SCI. To independently control the trajectory of each hindlimb after SCI, neurostimulation was applied alternately to the left and right motor cortex in

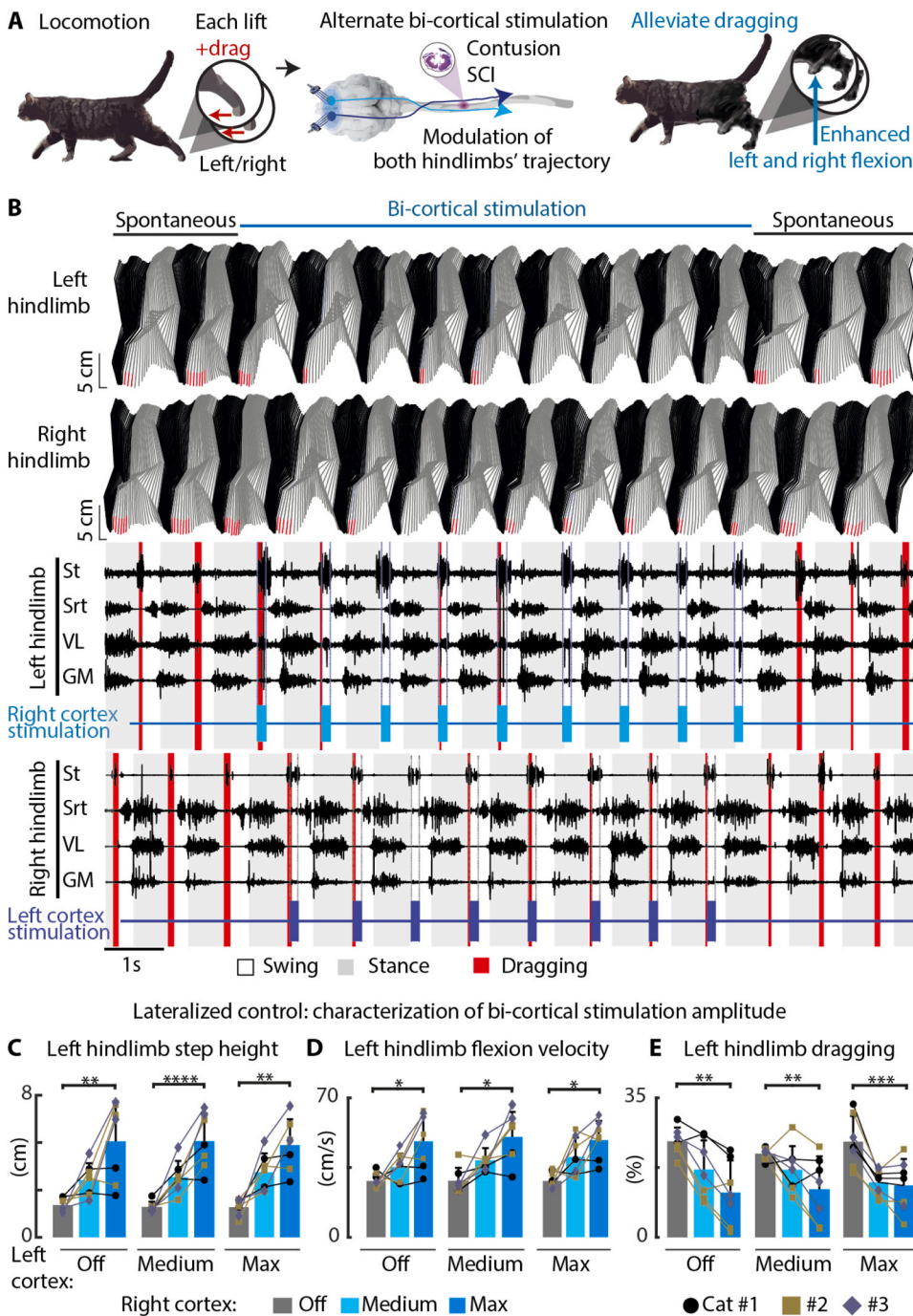


**Fig. 6.** Phase-coherent bi-cortical stimulation bilaterally modulated gait kinematics and reduced foot drop deficits after SCI. (A) Schematic representation of bi-cortical neurostimulation after an incomplete contusive SCI. Both cortices were stimulated alternately and in phase coherence with locomotion. (B) Stick diagram and EMG activity during spontaneous walking, with or without bi-cortical stimulation. During bi-cortical stimulation, the (C) left hindlimb step height, (D) left hindlimb flexion velocity and (E) left hindlimb dragging linearly modulated with increasing ICMS amplitudes applied to the right cortex, independently of the stimulation amplitude delivered to the homologous cortex.  $p$ : \*  $<0.05$ ; \*\*  $<0.01$ ; \*\*\*  $<0.001$ . St: semitendinosus, Srt: sartorius, VL: vastus lateralis, and GM: gastrocnemius medialis.

phase coherence with locomotion. In healthy cats, cortical stimulation elicited a variety of motor programs. In contrast, after SCI, the motor programs switched to a single stereotyped vertical flexion movement, which counteracted foot drag. Even in cats exhibiting an asymmetrical gait pattern, an optimal setting of stimulation parameters allowed to modulate trajectories of each hindlimb in a phase-dependent fashion. Cortical neuroprosthetic controllability re-emerged in synchrony with spontaneous recovery of locomotion.

The motor cortex plays a major role in voluntary control of locomotion (Drew et al., 2002). In cats and humans, damage to the motor cortex projections that are linked to the spinal circuits is associated with locomotor impairments (Barthelemy et al., 2010; Jiang and Drew, 1996). As previously observed in intact cats and rats, ICMS delivered during locomotion produces phase-dependent changes in locomotor

activity and controls contralateral hindlimb trajectories (Bonizzato and Martinez, 2021; Bretzner and Drew, 2005b; Fortier-Lebel et al., 2021). In intact and hemisected rats, phase-coherent cortical stimulation immediately enhanced contralateral hindlimb locomotor kinematics (Bonizzato and Martinez, 2021). Given its role in modulating locomotor output, the motor cortex is a target of choice for neuromodulation interventions intended to control limb movement during gait. The principal goal of this study was to select and enhance descending motor commands involved in locomotor control of both hindlimbs by bilaterally targeting the motor cortex.

In clinical settings, most SCIs are caused by closed traumas with displaced vertebral fractures and associated spinal contusion (N.S.C.I.S. C, 2019; RHI, 2018), which in most cases affect both legs and may induce asymmetrical locomotor deficits. In our cat model of contusive



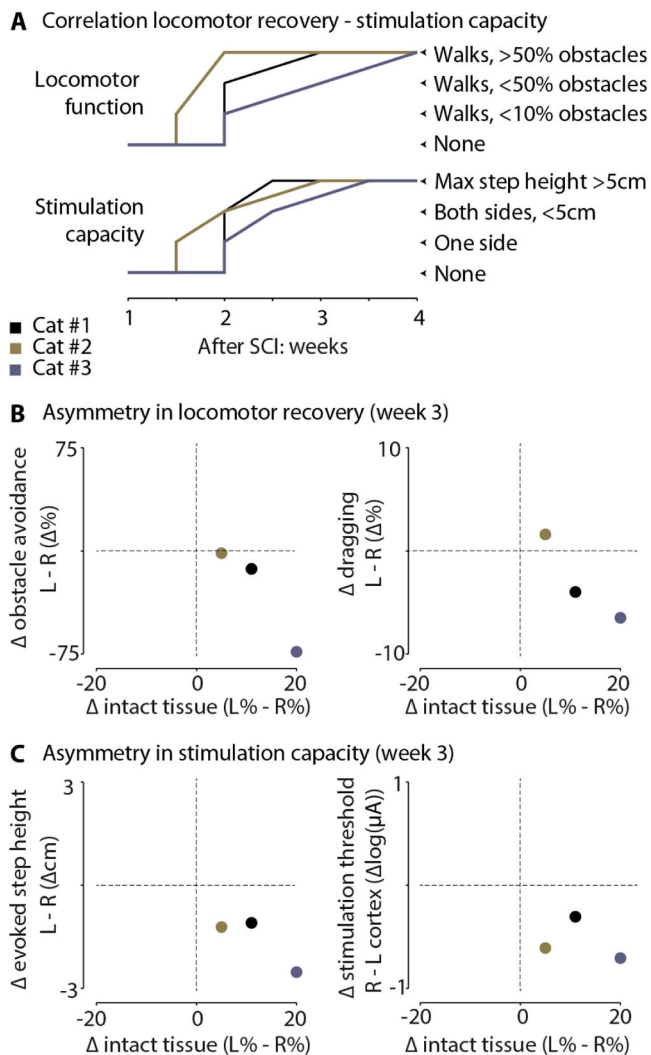


**Fig. 7.** The return of locomotion correlated with the re-emergence of cortically-induced gait modulation.

SCI, alternate bi-cortical neurostimulation had independent and limb-specific effects, allowing for the control of bilateral gait patterns by tuning optimal stimulation amplitude settings, even in cats that displayed an asymmetrical locomotor pattern.

Stimulation timing was essential to obtain an enhanced and integrated movement as well as to reduce foot drag after SCI. The optimal timing was synchronous with the contralateral hindlimb lift, which we defined as “phase-coherent” stimulation. Phase-coherent stimulation is an emerging paradigm in neuromodulation of locomotion. It is superior to continuous neurostimulation in animal and human studies involving spinal cord stimulation (Wagner et al., 2018; Wenger et al., 2016), cortical stimulation (Martinez, 2022), and even functional electrical stimulation of leg muscles (Donaldson et al., 2000). In the cat, ICMS applied to the motor cortex triggers flexion movements (Bretzner and Drew, 2005b; Fortier-Lebel et al., 2021), which naturally occur during the late stance and the beginning of the swing phase during locomotion. Here, we showed that the highest kinematic enhancement and largest reduction in foot drop deficit were observed when the stimulation was delivered in synchrony with the contralateral hindlimb lift. Consistently with previous studies (Bonizzato and Martinez, 2021; Bretzner and Drew, 2005b; Fortier-Lebel et al., 2021), ICMS only affected trajectories of the contralateral hindlimb.

Stimulation train duration played a smaller, but consistent role, in the control of the foot trajectory. As observed in other studies, short

trains of cortical stimulation tend to produce simple motor responses (Bretzner and Drew, 2005b; Brown and Martinez, 2018; Brown and Martinez, 2021), whereas long trains of stimulation may recruit functionally complex motor responses (Bretzner and Drew, 2005b; Brown et al., 2022; Brown and Teskey, 2014; Donoghue and Wise, 1982; Graziano et al., 2005). We tested different durations of stimulation trains, including short (50 ms) and longer stimuli (100, 150, 200 ms). We found that 100 ms trains enhanced natural movement, while limiting the total injected stimulation charge.

Before and after SCI, tuning stimulation amplitude allowed to achieve proportional modulation of kinematic parameters. The flexion velocity and step height were linearly correlated with increased stimulation amplitude and dragging was linearly reduced after SCI. The proportional stimulation effects were consistent with previous results in rats, both when quantifying cortical population engagement in spontaneous gait modulation (Bonizzato et al., 2018) and when applying cortical neurostimulation (Bonizzato and Martinez, 2021).

In intact cats, different stimulation sites evoked diverse motor synergies, which could selectively influence leg trajectories during locomotion. After SCI, stimulation of each cortical site resulted in a stereotyped modulation of swing characterized by a vertical flexion movement. This uniform response across subjects suggests that the diverse neurophysiological processes responsible for the spontaneous recovery of gait modulation converge on a singular compensatory strategy that strengthens this retrieved motor program over time. The compensation appears to be pragmatically aimed at one-dimensional control of vertical lift. The loss in movement variety evoked by ICMS could be the result of changes in excitability of the spinal circuits and could be determined, in great part, by the activity of the spinal central pattern generators (Dyson et al., 2014; Floeter et al., 1993; Perreault et al., 1994). Sensory and cortical inputs are integrated at the spinal level (Bretzner and Drew, 2005a; c), and converge onto specific interneuronal networks in the lumbar cord that modulate the activity of different group of synergetic muscles (Fleshman et al., 1988; Lundberg, 1964). Some studies show, in intact animals, that stimulation of the corticospinal pathway facilitates the excitatory effects of skin afferents in flexor motor neurons, while it facilitates the inhibitory effects of these afferents in extensor motor neurons (Lundberg and Voorhoeve, 1962). These interactions between sensory and cortical inputs are not homogeneous but rather specific: those are dramatically modified after SCI. Our previous studies in rats (Brown and Martinez, 2021) and cats (Martinez et al., 2012b) show that after SCI, some basic dynamical relationships between components of the central pattern generators (flexion, extension) are altered, as shown by a greater excitability within the flexor than the extensor rhythm generator. This increased excitability in the flexor oscillator may explain the inability of ICMS to recruit extensor circuits after SCI. ICMS may also recruit these flexor synergies through reticulospinal projections: the motor cortex holds direct connections with the reticular formation, which in turn modulates spinal locomotor circuits to produce phase-dependent motor responses according to the spinal circuit state (Drew, 1991; Drew and Rossignol, 1984; Dyson et al., 2014; Lemieux and Bretzner, 2019). Recruitment and upregulation of cortico-reticulo-spinal transmission is coherent with the cruder availability of motor control options after SCI. We do not discount the possibility of emergence of alternative movement programs when examining a broader range of less severe SCI cases. The motor cortex may have access to a more diverse range of motor programs following SCI if the injury preserves a greater number of descending connections.

Phase-coherent neuromodulation can be achieved with a variety of synchronization methods, including real-time kinematic tracking (Wenger et al., 2016) and data from tilt sensors or accelerometers (Dai et al., 1996; Weber et al., 2004). In this study, we used EMG pattern recognition to decode the extensor muscle activity preceding foot-strike, which was found to be as accurate as video tracking (Wenger et al., 2016), with the advantage of being portable (e.g., outside a laboratory setting). This method enabled delivery of stimulation within the

expected time window for optimal motor response with 83 % (intact state) and 88 % (after SCI) stimulation precision during uni-cortical stimulation, as well as a 97 % (intact state) and 98 % (after SCI) stimulation precision with bi-cortical stimulation. The superior pattern recognition performance with bi-cortical stimulation is explained by the regularization effects that phase-coherent cortical stimulation achieves during gait, which is associated with more organized stepping. Indeed, phase-coherent cortical stimulation reduced lift phase variability by increasing predictability of the lift movement (Bonizzato and Martinez, 2021). Bi-cortical neuromodulation applies this regularization effect to both hindlimbs, further benefiting the decoding precision.

Lesion profile analysis revealed that a variable proportion of supra-spinal fibers from cortical and brainstem centers remained intact after SCI. These bridges of intact fibers are essential to convey descending motor commands (generated in the motor cortex) to the lumbar spinal circuits that generate locomotor rhythms (Martinez and Rossignol, 2011). We found that the recovery of volitional walking assessed during the obstacle avoidance task paralleled the return of foot clearance. Although spinal plasticity is essential for the recovery of locomotor patterns (Martinez et al., 2011, 2012b; Martinez et al., 2013), the return of volitional walking involves reorganization of the circuits that propagate descending drive generated in the motor cortex (Brown and Martinez, 2019). After SCI, cortical (Bareyre et al., 2004; Bonizzato and Martinez, 2021; Brown and Martinez, 2018; Brown and Martinez, 2021), brainstem (Asboth et al., 2018; Fili et al., 2014), supraspinal (Bareyre et al., 2004; Fili and Schwab, 2015), and sublesional spinal circuits (Gossard et al., 2015) undergo extensive rewiring that contribute to recovery.

After SCI, we found that the recovery of locomotor control is correlated with the return of cortically evoked locomotor responses. As soon as the cats recovered stepping abilities, cortical stimulation evoked hindlimb movements. Since all cats displayed various levels of corticospinal sparing, residual corticospinal fibers may promote transmission of descending drive to spinal circuits. However, we previously demonstrated that this direct connectivity is not necessary for conveying cortical stimulation in rats with SCI that disrupted all corticospinal fibers (Bonizzato and Martinez, 2021). We and others (Asboth et al., 2018; Bonizzato and Martinez, 2021) have suggested that the upregulation of indirect cortico-reticulospinal pathways, which remain partially spared in our cats, may provide a neural substrate for relaying cortical drive. Considering that cortical stimulation only elicited flexion movements after SCI, the modulation of the flexion related outputs of pattern generation by ICMS is likely gated, in a phase-dependent manner, by spared corticospinal or cortico-reticulospinal pathways (Bretzner and Drew, 2005b; Drew, 1991; Drew and Rossignol, 1984; Dyson et al., 2014; Fortier-Lebel et al., 2021; Lemieux and Bretzner, 2019). Other pathways may also be involved. For example, the rubrospinal tract is known to share functional properties with the corticospinal tract during both regulation of fine contralateral forelimb movements (Alstermark et al., 1987; Pettersson et al., 2000) and modifications of contralateral leg trajectories (Lavoie and Drew, 2002; Rho et al., 1999). Given the specific effects of cortical stimulation in modulating contralateral movements in real-time, it is unlikely that interhemispheric communication significantly contributed to mediating cortical stimulation effect over locomotor output (Brus-Ramer et al., 2009). Direct neuronal activations likely involve localized networks, since current propagation of ICMS depends on its intensity (Stoney et al., 1968). Maximal stimuli amplitudes were mostly within the range of 100–300  $\mu$ A, and never exceeded the 500  $\mu$ A threshold, which primarily corresponds to sub-millimeter excitation propagation, based on the Stoney equation. Additional mechanistic studies are needed to unveil the pathways through which ICMS exerts its effects over lumbar spinal circuits.

The efficacy of cortical neuroprosthesis in piloting locomotor movements and immediately alleviating bilateral locomotor deficits is here demonstrated in a clinically relevant model of contusive SCI. This research promotes the use of cortical neuromodulation as a movement

assistance tool for motor rehabilitation. Similar to our animal model of contusive SCI, individuals with SCI exhibit various lesion and recovery profiles (Frigon, 2015), requiring personalized interventions. Our work has shown that cortical neuromodulation exerted a proportional control of foot trajectories and specifically targeted each hindlimb. Modulating the intensity of stimuli in the left and right cortex allowed tuning step height symmetry. Cortical neuroprosthetic approaches may efficiently serve individuals with incomplete SCI or subcortical stroke, who display various degrees of motor deficits, including foot drop and an asymmetrical gait pattern (Mignardot et al., 2017). In the context of rehabilitation, the recovery of voluntary function may be accelerated and enhanced by neuromodulation approaches that repeatedly select, control, and train complex whole-limb lifting movements. Even though implantation and explantation of intracortical probes such as Utah arrays in animals and humans cause minor tissue damage, apart from reactive gliosis (Bullard et al., 2020), the invasive nature of cortical probes remains a hurdle and a potential limitation of our approach. New electrode designs, such as intravascular electrodes (Oxley et al., 2021) may mitigate these problems. In addition, non-surgical approaches, including transcranial magnetic stimulation (Benito et al., 2012; Kumru et al., 2016; Raithatha et al., 2016) have been explored in experimental clinical protocols (Dixon et al., 2016; Jo and Perez, 2020). If results are consolidated, then similar protocols may be expanded for broader clinical use. Further experiments are required to establish the trade-off between interface invasiveness and stimulation efficacy. However, it is worth considering that this technique is not more invasive than deep brain stimulation, which has been available for decades and is considered safe for alleviating symptoms of Parkinson's disease (Liu et al., 2015; Stefani et al., 2007). Moreover, deep brain stimulation is currently being tested in humans with SCI (clinicaltrials.gov ID NCT03053791). As for these approaches, biocompatibility studies are necessary to assess inflammatory responses induced by both our neural interface and chronic delivery of current (Rajan et al., 2015). In this study, after cortical implantation, we found no motor deficits nor any side effects such as pain.

A major advantage of our animal model is that spinal contusion better reflects the mechanism of injury in humans, as opposed to spinal sections. However, this animal model also has several limitations. First, re-expression of locomotion after severe SCI in cats is more complete compared to humans (Barbeau and Rossignol, 1987; Harnie et al., 2019; Nadeau et al., 2010). Spontaneous locomotor recovery in both humans and cats is mediated by several non-exclusive mechanisms, however spinal locomotor circuits may be more autonomous and plastic in the cat (Barbeau and Rossignol, 1987; Harnie et al., 2019; Martinez et al., 2011, 2012a; b; Martinez et al., 2013), since re-expression of spinal locomotion in humans also requires enabling factors (Angeli et al., 2014; Remy-Neris et al., 1999; Rowald et al., 2022). Nevertheless, the greater reliance of humans on corticospinal input for locomotion (Field-Fote et al., 2017) only increases the relevance of our supra-lesional stimulation strategy to restore locomotion following an incomplete SCI. Second, the ability of ICMS to recruit extension synergies was lost after SCI, suggesting a specific recruitment of spinal flexion synergies by ICMS in our cat model. This result contrasts with our recent study in the rat model of spinal hemisection showing that ICMS delivered to the ipsilesional motor cortex promoted a bilateral synergy, whereby the elevation of the contralateral hindlimb was accompanied by ipsilateral hindlimb extension (Massai et al., 2021). The inability to modulate extensor activity might be due to various experimental factors, including the lesion model (lateralized versus bilateral SCI) and/or functional organization of motor circuits that might slightly differ between rats and cats. If similar results are found in humans, the potential use of our cortical neuroprosthesis could be limited when attempting to increase extensor activity. As alternative strategies to target both flexor and extensor synergies, phase-dependent stimulation of the spinal circuits or reticular formation have been shown to recruit various spinal synergies (Drew, 1991; Lemieux and Bretzner, 2019; Rowald et al., 2022; Wagner et al.,

2018; Wenger et al., 2016). Those strategies could also be combined to maximize motor output and foster reorganisation of the whole motor system. Third, cats exhibit significantly less upper motoneuron signs following SCI, notably less spasticity. Despite a few studies, which have shown that repetitive transcranial magnetic stimulation may decrease spasticity in individuals with incomplete SCI (Benito et al., 2012; Kumru et al., 2010), the underlying neurophysiological mechanisms contributing to this process are still not understood. Consequently, a comprehensive examination of the impact of cortical stimulation on spinal plasticity and excitability is necessary. Lastly, this study only focused on immediate modulation of locomotion, without assessing the long-term effects of cortical stimulation on locomotor recovery. While supported by rat lesion models focused on elucidating the mechanisms of cortical stimulation (Bonizzato and Martinez, 2021; Carmel et al., 2010; Carmel et al., 2014), the long-term effects of bi-cortical neuromodulation on recovery from clinically relevant contusive SCI will require additional studies.

## Funding

This work was supported by the Natural Sciences and Engineering Research Council of Canada (RGPIN-2015-03860), the TransMedTech Institute and the Morton Cure Paralysis Fund, US. M.M. was supported by a salary award from the Fonds de Recherche Québec Santé (FRQS). M.D. was supported by scholarships from the FRQS and the Université de Montréal. M.B. was supported by the Institut de valorisation des données (IVADO), the TransMedTech Institute and a departmental fellowship in memory of Tomás A. Reader.

## CRediT authorship contribution statement

Conceptualization: MB, MM; Methodology: MD, MB, HDM, NFL, MM; Investigation: MD, MB, HDM, NFL, MM; Visualization: MD, MB, HDM, MM; Funding acquisition: MM; Project administration: MM; Supervision: MM; Writing – original draft: MD, MM; Writing – review & editing: MD, MB, HDM, NFL, MM.

## Declaration of Competing Interest

M.B. and M.M. filed a patent application (U.S. No. 62/880,364) covering a device that allows one to perform cortical stimulation during movement. They are also shareholders of a start-up company focused on developing neurostimulation technologies.

## Data Availability

Data will be made available on request.

## Acknowledgements

The authors would like to thank Gaëlle Forest St-Onge, Alexandre Sheasby, Rania Lejri, David Bergeron, and Anne-Catherine Chouinard for their participation in data processing; Marjolaine Homier, Stéphane Ménard, Raphaël Santamaria, and the staff at the Division des Animaleries for supporting our animal care.

## Appendix A. Supporting information

Supplementary data associated with this article can be found in the online version at doi:10.1016/j.pneurobio.2023.102492.

## References

Ahuja, C.S., Wilson, J.R., Nori, S., Kotter, M.R.N., Druschel, C., Curt, A., Fehlings, M.G., 2017. Traumatic spinal cord injury. *Nat. Rev. Dis. Prim.* 3, 17018.

- Alstermark, B., Lundberg, A., Pettersson, L.-G., Tantisira, B., Walkowska, M., 1987. Motor recovery after serial spinal cord lesions of defined descending pathways in cats. *Neurosci. Res.* 5, 68–73.
- Angeli, C.A., Edgerton, V.R., Gerasimenko, Y.P., Harkema, S.J., 2014. Altering spinal cord excitability enables voluntary movements after chronic complete paralysis in humans. *Brain* 137, 1394–1409.
- Asboth, L., Friedli, L., Beauparlant, J., Martinez-Gonzalez, C., Anil, S., Rey, E., Baud, L., Pidpruzhnykova, G., Anderson, M.A., Shkorbatova, P., Batti, L., Pages, S., Kreider, J., Schneider, B.L., Barraud, Q., Courtine, G., 2018. Cortico-reticulo-spinal circuit reorganization enables functional recovery after severe spinal cord contusion. *Nat. Neurosci.* 21, 576–588.
- Barbeau, H., Rossignol, S., 1987. Recovery of locomotion after chronic spinalization in the adult cat. *Brain Res.* 412, 84–95.
- Bareyre, F.M., Kerschensteiner, M., Raineteau, O., Mettenleiter, T.C., Weinmann, O., Schwab, M.E., 2004. The injured spinal cord spontaneously forms a new intraspinal circuit in adult rats. *Nat. Neurosci.* 7, 269–277.
- Barthelemy, D., Willerslev-Olsen, M., Lundell, H., Conway, B.A., Knudsen, H., Biering-Sorensen, F., Nielsen, J.B., 2010. Impaired transmission in the corticospinal tract and gait disability in spinal cord injured persons. *J. Neurophysiol.*
- Benito, J., Kumru, H., Murillo, N., Costa, U., Medina, J., Tormos, J.M., Pascual-Leone, A., Vidal, J., 2012. Motor and gait improvement in patients with incomplete spinal cord injury induced by high-frequency repetitive transcranial magnetic stimulation. *Top. Spinal Cord. Inj. Rehabil.* 18, 106–112.
- Bonizzato, M., Martinez, M., 2021. An intracortical neuroprosthesis immediately alleviates walking deficits and improves recovery of leg control after spinal cord injury. *Sci. Transl. Med.* 13, 1–14.
- Bonizzato, M., Pidpruzhnykova, G., DiGiovanna, J., Shkorbatova, P., Pavlova, N., Micera, S., Courtine, G., 2018. Brain-controlled modulation of spinal circuits improves recovery from spinal cord injury. *Nat. Commun.* 9, 3015.
- Bretzner, F., Drew, T., 2005a. Changes in corticospinal efficacy contribute to the locomotor plasticity observed following unilateral cutaneous denervation of the hindpaw in the cat. *J. Neurophysiol.* 94, 2911–2927.
- Bretzner, F., Drew, T., 2005b. Contribution of the motor cortex to the structure and the timing of hindlimb locomotion in the cat: a microstimulation study. *J. Neurophysiol.* 94, 657–672.
- Bretzner, F., Drew, T., 2005c. Motor cortical modulation of cutaneous reflex responses in the hindlimb of the intact cat. *J. Neurophysiol.* 94, 673–687.
- Brown, A.R., Martinez, M., 2018. Ipsilesional motor cortex plasticity participates in spontaneous hindlimb recovery after lateral hemisection of the thoracic spinal cord in the rat. *J. Neurosci.* 38, 9977–9988.
- Brown, A.R., Martinez, M., 2019. From cortex to cord: motor circuit plasticity after spinal cord injury. *Neural Regen. Res.* 14, 2054.
- Brown, A.R., Martinez, M., 2021. Chronic inactivation of the contralesional hindlimb motor cortex after thoracic spinal cord hemisection impedes locomotor recovery in the rat. *Exp. Neurol.* 343.
- Brown, A.R., Teskey, G.C., 2014. Motor cortex is functionally organized as a set of spatially distinct representations for complex movements. *J. Neurosci.* 34, 13574–13585.
- Brown, A.R., Mitra, S., Teskey, G.C., Boychuk, J.A., 2022. Complex forelimb movements and cortical topography evoked by intracortical microstimulation in male and female mice. *Cereb. Cortex.*
- Brus-Ramer, M., Carmel, J.B., Martin, J.H., 2009. Motor cortex bilateral motor representation depends on subcortical and interhemispheric interactions. *J. Neurosci.* 29, 6196–6206.
- Bullard, A.J., Hutchison, B.C., Lee, J., Chestek, C.A., Patil, P.G., 2020. Estimating risk for future intracranial, fully implanted, modular neuroprosthetic systems: a systematic review of hardware complications in clinical deep brain stimulation and experimental human intracortical arrays. *Neuromodulation* 23, 411–426.
- Carmel, J.B., Berrol, L.J., Brus-Ramer, M., Martin, J.H., 2010. Chronic electrical stimulation of the intact corticospinal system after unilateral injury restores skilled locomotor control and promotes spinal axon outgrowth. *J. Neurosci.* 30, 10918–10926.
- Carmel, J.B., Kimura, H., Martin, J.H., 2014. Electrical stimulation of motor cortex in the uninjured hemisphere after chronic unilateral injury promotes recovery of skilled locomotion through ipsilateral control. *J. Neurosci.* 34, 462–466.
- Dai, R., Stein, R.B., Andrews, B.J., James, K.B., Wieler, M., 1996. Application of tilt sensors in functional electrical stimulation. *IEEE Trans. Rehabil. Eng.* 4, 63–72.
- D'Angelo, G., Thibaudier, Y., Telonio, A., Hurteau, M.F., Kuczyński, V., Dambreville, C., Frigon, A., 2014. Modulation of phase durations, phase variations and temporal coordination of the four limbs during quadrupedal split-belt locomotion in intact adult cats. *J. Neurophysiol.* 112, 1825–1837.
- Delivet-Mongrain, H., Dea, M., Gossard, J.P., Rossignol, S., 2020. Recovery of locomotion in cats after severe contusion of the low thoracic spinal cord. *J. Neurophysiol.* 123, 1504–1525.
- DiGiovanna, J., Dominici, N., Friedli, L., Rigosa, J., Duis, S., Kreider, J., Beauparlant, J., van den Brand, R., Schieppati, M., Micera, S., Courtine, G., 2016. Engagement of the rat hindlimb motor cortex across natural locomotor behaviors. *J. Neurosci.* 36, 10440–10455.
- Ditunno, P.L., Patrick, M., Stineman, M., Ditunno, J.F., 2008. Who wants to walk? Preferences for recovery after SCI: a longitudinal and cross-sectional study. *Spinal Cord.* 46, 500–506.
- Dixon, L., Ibrahim, M.M., Santora, D., Knikou, M., 2016. Paired associative transspinal and transcortical stimulation produces plasticity in human cortical and spinal neuronal circuits. *J. Neurophysiol.* 116, 904–916.



- Donaldson, N., Perkins, T.A., Fitzwater, R., Wood, D.E., Middleton, F., 2000. FES cycling may promote recovery of leg function after incomplete spinal cord injury. *Spinal Cord* 38, 680–682.
- Donoghue, J.P., Wise, S.P., 1982. The motor cortex of the rat: cytoarchitecture and microstimulation mapping. *J. Comp. Neurol.* 212, 76–88.
- Drew, T., 1991. Functional organization within the medullary reticular formation of the intact unanesthetized cat. III. Microstimulation during locomotion. *J. Neurophysiol.* 66, 919–938.
- Drew, T., 1993. Motor cortical activity during voluntary gait modifications in the cat. I. Cells related to the forelimbs. *J. Neurophysiol.* 70, 179–199.
- Drew, T., Rossignol, S., 1984. Phase-dependent responses evoked in limb muscles by stimulation of medullary reticular formation during locomotion in thalamic cats. *J. Neurophysiol.* 52, 653–675.
- Drew, T., Jiang, W., Widajewicz, W., 2002. Contributions of the motor cortex to the control of the hindlimbs during locomotion in the cat. *Brain Res. Rev.* 40, 178–191.
- Dyson, K.S., Miron, J.P., Drew, T., 2014. Differential modulation of descending signals from the reticulospinal system during reaching and locomotion. *J. Neurophysiol.* 112, 2505–2528.
- Field-Fote, E.C., Yang, J.F., Basso, D.M., Gorassini, M.A., 2017. Supraspinal control predicts locomotor function and forecasts responsiveness to training after spinal cord injury. *J. Neurotrauma* 34, 1813–1825.
- Filli, L., Schwab, M.E., 2015. Structural and functional reorganization of propriospinal connections promotes functional recovery after spinal cord injury. *Neural Regen. Res.* 10, 509–513.
- Filli, L., Engmann, A.K., Zorner, B., Weinmann, O., Moraitis, T., Gullo, M., Kasper, H., Schneider, R., Schwab, M.E., 2014. Bridging the gap: a reticulo-propriospinal detour bypassing an incomplete spinal cord injury. *J. Neurosci.* 34, 13399–13410.
- Fleshman, J.W., Rudomin, P., Burke, R.E., 1988. Supraspinal control of a short-latency cutaneous pathway to hindlimb motoneurons. *Exp. Brain Res.* 69, 449–459.
- Floeter, M.K., Sholomenko, G.N., Gossard, J.-P., Burke, R.E., 1993. Disynaptic excitation from the medial longitudinal fasciculus to lumbosacral motoneurons: modulation by repetitive activation, descending pathways, and locomotion. *Exp. Brain Res.* 92, 407–419.
- Fortier-Lebel, N., Nakajima, T., Yahiaoui, N., Drew, T., 2021. Microstimulation of the premotor cortex of the cat produces phase-dependent changes in locomotor activity. *Cereb. Cortex*.
- Frigon, A., 2015. Responders and non-responders in motor control research: a framework to study physiological mechanisms of inter-individual variability. *Clin. Neurophysiol.* 126, 1284–1285.
- Frigon, A., Thibaudier, Y., Hurteau, M.F., 2015. Modulation of forelimb and hindlimb muscle activity during quadrupedal tied-belt and split-belt locomotion in intact cats. *Neuroscience* 290, 266–278.
- Frigon, A., Desrochers, E., Thibaudier, Y., Hurteau, M.F., Dambreville, C., 2017. Left-right coordination from simple to extreme conditions during split-belt locomotion in the chronic spinal adult cat. *J. Physiol.* 595, 341–361.
- Ghosh, S., 1997. Identification of motor areas of the cat cerebral cortex based on studies of cortical stimulation and corticospinal connections. *J. Comp. Neurol.* 380, 191–214.
- Gossard, J.P., Delivet-Mongrain, H., Martinez, M., Kundu, A., Escalona, M., Rossignol, S., 2015. Plastic changes in lumbar locomotor networks after a partial spinal cord injury in cats. *J. Neurosci.* 35, 9446–9455.
- Graziano, M.S., Affalo, T.N., Cooke, D.F., 2005. Arm movements evoked by electrical stimulation in the motor cortex of monkeys. *J. Neurophysiol.* 94, 4209–4223.
- Grillner, S., Zangger, P., 1979. On the central generation of locomotion in the low spinal cat. *Exp. Brain Res.* 34, 241–261.
- Harnie, J., Doelman, A., de Vette, E., Audet, J., Desrochers, E., Gaudreault, N., Frigon, A., 2019. The recovery of standing and locomotion after spinal cord injury does not require task-specific training. *Elife* 8.
- Hatanaka, N., Nambu, A., Yamashita, A., Takada, M., Tokuno, H., 2001. Somatotopic arrangement and corticocortical inputs of the hindlimb region of the primary motor cortex in the macaque monkey. *Neurosci. Res.* 40, 9–22.
- Jiang, W., Drew, T., 1996. Effects of bilateral lesions of the dorsolateral funiculi and dorsal columns at the level of the low thoracic spinal cord on the control of locomotion in the adult cat: I. Treadmill walking. *J. Neurophysiol.* 76, 849–866.
- Jo, H.J., Perez, M.A., 2020. Corticospinal-motor neuronal plasticity promotes exercise-mediated recovery in humans with spinal cord injury. *Brain* 143, 1368–1382.
- Jordan, L.M., Liu, J., Hedlund, P.B., Akay, T., Pearson, K.G., 2008. Descending command systems for the initiation of locomotion in mammals. *Brain Res. Rev.* 57, 183–191.
- Kiehn, O., 2006. Locomotor circuits in the mammalian spinal cord. *Annu. Rev. Neurosci.* 29, 279–306.
- Kumru, H., Murillo, N., Vidal, S.J., Valls-Sole, J., Edwards, D., Pelayo, R., Valero-Cabre, A., Tormos, J.M., Pascual-Leone, A., 2010. Reduction of spasticity with repetitive transcranial magnetic stimulation in patients with spinal cord injury. *Neurorehabil. Neural Repair* 24, 435–441.
- Kumru, H., Murillo, N., Benito-Penalva, J., Tormos, J.M., Vidal, J., 2016. Transcranial direct current stimulation is not effective in the motor strength and gait recovery following motor incomplete spinal cord injury during Lokomat(R) gait training. *Neurosci. Lett.* 620, 143–147.
- Lavoie, S., Drew, T., 2002. Discharge characteristics of neurons in the red nucleus during voluntary gait modifications: A comparison with the motor cortex. *J. Neurophysiol.* 88, 1791–1814.
- Lecomte, C.G., Audet, J., Harnie, J., Frigon, A., 2021. A validation of supervised deep learning for gait analysis in the cat. *Front. Neuroinform* 15, 712623.
- Lemieux, M., Bretzner, F., 2019. Glutamatergic neurons of the gigantocellular reticular nucleus shape locomotor pattern and rhythm in the freely behaving mouse. *PLoS Biol.* 17, e2003880.
- Liu, H.G., Zhang, K., Yang, A.C., Zhang, J.G., 2015. Deep brain stimulation of the subthalamic and pedunculopontine nucleus in a patient with Parkinson's disease. *J. Korean Neurosurg. Soc.* 57, 303–306.
- Lundberg, A., 1964. Supraspinal control of transmission in reflex paths to motoneurons and primary afferents. *Prog. Brain Res.* 12, 197–221.
- Lundberg, A., Voorhoeve, P., 1962. Effects from the pyramidal tract on spinal reflex arcs. *Acta Physiol. Scand.* 56, 201–219.
- Martinez, M., 2022. Targeting the motor cortex to restore walking after incomplete spinal cord injury. *Neural Regen. Res.* 17, 1489–1490.
- Martinez, M., Rossignol, S., 2011. Changes in CNS structures after spinal cord lesions implications for BMI. *Prog. Brain Res.* 194, 191–202.
- Martinez, M., Delivet-Mongrain, H., Leblond, H., Rossignol, S., 2011. Recovery of hindlimb locomotion after incomplete spinal cord injury in the cat involves spontaneous compensatory changes within the spinal locomotor circuitry. *J. Neurophysiol.* 106, 1969–1984.
- Martinez, M., Delivet-Mongrain, H., Leblond, H., Rossignol, S., 2012a. Effect of locomotor training in completely spinalized cats previously submitted to a spinal hemisection. *J. Neurosci.* 32, 10961–10970.
- Martinez, M., Delivet-Mongrain, H., Leblond, H., Rossignol, S., 2012b. Incomplete spinal cord injury promotes durable functional changes within the spinal locomotor circuitry. *J. Neurophysiol.* 108, 124–134.
- Martinez, M., Delivet-Mongrain, H., Rossignol, S., 2013. Treadmill training promotes spinal changes leading to locomotor recovery after partial spinal cord injury in cats. *J. Neurophysiol.* 109, 2909–2922.
- Massai, E., Bonizzato, M., Martinez, M., 2021. Cortical neuroprosthesis-mediated functional ipsilateral control of locomotion in rats with incomplete spinal cord injury. *bioRxiv*. <https://doi.org/10.1101/2023.03.01.530610>, 2023.03.01.530610.
- Mathis, A., Mamidanna, P., Cury, K.M., Abe, T., Murthy, V.N., Mathis, M.W., Bethge, M., 2018. DeepLabCut: markerless pose estimation of user-defined body parts with deep learning. *Nat. Neurosci.* 21, 1281–1289.
- Metz, G.A., Dietz, V., Schwab, M.E., Van de Meent, H., 1998. The effects of unilateral pyramidal tract section on hindlimb motor performance in the rat. *Behav. Brain Res.* 96, 37–46.
- Mignardot, J.B., Goff, Le, van den Brand, C.G., Capogrosso, R., Fumeaux, M., Vallery, N., Anil, H., Lanini, S., Fodor, J., Eberle, I., Ijspeert, G., Schurch, A., Curt, B., Carda, A., Bloch, S., von Zitzewitz, J., Courtine, G., 2017. A multidirectional gravity-assist algorithm that enhances locomotor control in patients with stroke or spinal cord injury. *Sci. Transl. Med.* 9.
- N.S.C.I.S.C., 2019. Spinal Cord Injury Facts and Figures at a Glance. *The National Spinal Cord Injury Database Birmingham, AL*.
- Nadeau, S., Jacquemin, G., Fournier, C., Lamarre, Y., Rossignol, S., 2010. Spontaneous motor rhythms of the back and legs in a patient with a complete spinal cord transection. *Neurorehabil. Neural Repair* 24, 377–383.
- Neafsey, E.J., Bold, E.L., Haas, G., Hurley-Gius, K.M., Quirk, G., Sievert, C.F., Terreberry, R.R., 1986. The organization of the rat motor cortex: a microstimulation mapping study. *Brain Res.* 396, 77–96.
- Nieoullon, A., Rispal-Padel, L., 1976. Somatotopic localization in cat motor cortex. *Brain Res.* 105, 405–422.
- Oxley, T.J., Yoo, P.E., Rind, G.S., Ronayne, S.M., Lee, C.M.S., Bird, C., Hampshire, V., Sharma, R.P., Morokoff, A., Williams, D.L., MacIsaac, C., Howard, M.E., Irving, L., Vrljic, I., Williams, C., John, S.E., Weissenborn, F., Dzenko, M., Balabanski, A.H., Friedenberg, D., Burkitt, A.N., Wong, Y.T., Drummond, K.J., Desmond, P., Weber, D., Denison, T., Hochberg, L.R., Mathers, S., O'Brien, T.J., May, C.N., Mocco, J., Grayden, D.B., Campbell, B.C.V., Mitchell, P., Opie, N.L., 2021. Motor neuroprosthesis implanted with neurointerventional surgery improves capacity for activities of daily living tasks in severe paralysis: first in-human experience. *J. Neurointerv. Surg.* 13, 102–108.
- Perreault, M.-C., Rossignol, S., Drew, T., 1994. Microstimulation of the medullary reticular formation during fictive locomotion. *J. Neurophysiol.* 71, 229–245.
- Pettersson, L.G., Blagovestchenski, E., Perfiliev, S., Krasnochokova, E., Lundberg, A., 2000. Recovery of food-taking in cats after lesions of the corticospinal (complete) and rubrospinal (complete and incomplete) tracts. *Neurosci. Res.* 38, 109–112.
- Prochazka, A., Gritsenko, V., Yakovenko, S., 2002. Sensory control of locomotion: reflexes versus higher-level control. *Adv. Exp. Med. Biol.* 508, 357–367.
- Raithatha, R., Carrico, C., Powell, E.S., Westgate, P.M., Chelette, II, K.C., Lee, K., Dunsmore, L., Salles, S., Sawaki, L., 2016. Non-invasive brain stimulation and robot-assisted gait training after incomplete spinal cord injury: a randomized pilot study. *NeuroRehabilitation* 38, 15–25.
- Rajan, A.T., Boback, J.L., Dammann, J.F., Tenore, F.V., Wester, B.A., Otto, K.J., Gaunt, R. A., Bensmaia, S.J., 2015. The effects of chronic intracortical microstimulation on neural tissue and fine motor behavior. *J. Neural Eng.* 12, 066018.
- Remy-Neris, O., Barbeau, H., Daniel, O., Boiteau, F., Bussel, B., 1999. Effects of intrathecal clonidine injection on spinal reflexes and human locomotion in incomplete paraplegic subjects. *Exp. Brain Res.* 129, 433–440.
- RHI (2018) Rick Hansen Spinal Cord Injury Registry - A look at traumatic spinal cord injury in Canada in 2017. Vancouver, BC.
- Rho, M.J., Lavoie, S., Drew, T., 1999. Effects of red nucleus microstimulation on the locomotor pattern and timing in the intact cat: a comparison with the motor cortex. *J. Neurophysiol.* 81, 2297–2315.
- Rossignol, S., Dubuc, R., Gossard, J.P., 2006. Dynamic sensorimotor interactions in locomotion. *Physiol. Rev.* 86, 89–154.
- Rowald, A., Komi, S., Demesmaeker, R., Baaklini, E., Hernandez-Charpak, S.D., Paoles, E., Montanaro, H., Cassara, A., Becce, F., Lloyd, B., Newton, T., Ravier, J., Kinany, N., D'Ercole, M., Paley, A., Hankov, N., Varescon, C., McCracken, L., Vat, M., Caban, M., Watrin, A., Jacquet, C., Bole-Feysot, L., Harte, C., Lorach, H., Galvez, A., Tschopp, M., Herrmann, N., Wacker, M., Geernaert, L., Fodor, I., Radevich, V., Van

- Den Keybus, K., Eberle, G., Pralong, E., Roulet, M., Ledoux, J.B., Fornari, E., Mandija, S., Mattera, L., Martuzzi, R., Nazarian, B., Benkler, S., Callegari, S., Greiner, N., Fuhrer, B., Froeling, M., Buse, N., Denison, T., Buschman, R., Wende, C., Ganty, D., Bakker, J., Delattre, V., Lambert, H., Minassian, K., van den Berg, C.A.T., Kavounoudias, A., Micera, S., Van De Ville, D., Barraud, Q., Kurt, E., Kuster, N., Neufeld, E., Capogrosso, M., Asboth, L., Wagner, F.B., Bloch, J., Courtine, G., 2022. Activity-dependent spinal cord neuromodulation rapidly restores trunk and leg motor functions after complete paralysis. *Nat. Med.* 28, 260–271.
- Sahrmann, S.A., Clare, M.H., Montgomery, E.B., Jr, Landau, W.M., 1984. Motor cortical neuronal activity patterns in monkeys performing several force tasks at the ankle. *Brain Res.* 310, 55–66.
- Seong, H.Y., Cho, J.Y., Choi, B.S., Min, J.K., Kim, Y.H., Roh, S.W., Kim, J.H., Jeon, S.R., 2014. Analysis on bilateral hindlimb mapping in motor cortex of the rat by an intracortical microstimulation method. *J. Korean Med. Sci.* 29, 587–592.
- Stefani, A., Lozano, A.M., Peppe, A., Stanzione, P., Galati, S., Tropepi, D., Pierantozzi, M., Brusa, L., Scarnati, E., Mazzone, P., 2007. Bilateral deep brain stimulation of the pedunculopontine and subthalamic nuclei in severe Parkinson's disease. *Brain* 130, 1596–1607.
- Stoney Jr., S.D., Thompson, W.D., Asanuma, H., 1968. Excitation of pyramidal tract cells by intracortical microstimulation: effective extent of stimulating current. *J. Neurophysiol.* 31, 659–669.
- Topka, H., Cohen, L.G., Cole, R.A., Hallett, M., 1991. Reorganization of corticospinal pathways following spinal cord injury. *Neurology* 41, 1276–1283.
- Urbán, M.A., Royston, D.A., Weber, D.J., Boninger, M.L., Collinger, J.L., 2019. What is the functional relevance of reorganization in primary motor cortex after spinal cord injury? *Neurobiol. Dis.* 121, 286–295.
- Wagner, F.B., Mignardot, J.B., Le Goff-Mignardot, C.G., Demesmaeker, R., Komi, S., Capogrosso, M., Rowald, A., Seanez, I., Caban, M., Pirondini, E., Vat, M., McCracken, L.A., Heimgartner, R., Fodor, I., Watrin, A., Seguin, P., Paoles, E., Van Den Keybus, K., Eberle, G., Schurch, B., Pralong, E., Becce, F., Prior, J., Buse, N., Buschman, R., Neufeld, E., Kuster, N., Carda, S., von Zitzewitz, J., Delattre, V., Denison, T., Lambert, H., Minassian, K., Bloch, J., Courtine, G., 2018. Targeted neurotechnology restores walking in humans with spinal cord injury. *Nature* 563, 65–71.
- Weber, D.J., Stein, R.B., Chan, K.M., Loeb, G.E., Richmond, F.J., Rolf, R., James, K., Chong, S.L., Thompson, A.K., Misiasek, J., 2004. Functional electrical stimulation using microstimulators to correct foot drop: a case study. *Can. J. Physiol. Pharm.* 82, 784–792.
- Wenger, N., Moraud, E.M., Gandar, J., Musienko, P., Capogrosso, M., Baud, L., Le Goff, C. G., Barraud, Q., Pavlova, N., Dominici, N., Minev, I.R., Asboth, L., Hirsch, A., Duis, S., Kreider, J., Mortera, A., Haverbeck, O., Kraus, S., Schmitz, F., DiGiovanna, J., van den Brand, R., Bloch, J., Detemple, P., Lacour, S.P., Bezard, E., Micera, S., Courtine, G., 2016. Spatiotemporal neuromodulation therapies engaging muscle synergies improve motor control after spinal cord injury. *Nat. Med.* 22, 138–145.
- Widajewicz, W., Kably, B., Drew, T., 1994. Motor cortical activity during voluntary gait modifications in the cat. II. Cells related to the hindlimbs. *J. Neurophysiol.* 72, 2070–2089.
- Zehr, E.P., Stein, R.B., 1999. What functions do reflexes serve during human locomotion? *Prog. Neurobiol.* 58, 185–205.